UCRL-11947

University of California

Ernest O. Lawrence Radiation Laboratory

TWO-WEEK LOAN COPY

This is a Library Circulating Copy which may be borrowed for two weeks. For a personal retention copy, call Tech. Info. Division, Ext. 5545

(d, α) REACTIONS ON C^{12}, N^{14} AND O^{16} INDUCED BY 24 MeV DEUTERONS

Berkeley, California

DISCLAIMER

This document was prepared as an account of work sponsored by the United States Government. While this document is believed to contain correct information, neither the United States Government nor any agency thereof, nor the Regents of the University of California, nor any of their employees, makes any warranty, express or implied, or assumes any legal responsibility for the accuracy, completeness, or usefulness of any information, apparatus, product, or process disclosed, or represents that its use would not infringe privately owned rights. Reference herein to any specific commercial product, process, or service by its trade name, trademark, manufacturer, or otherwise, does not necessarily constitute or imply its endorsement, recommendation, or favoring by the United States Government or any agency thereof, or the Regents of the University of California. The views and opinions of authors expressed herein do not necessarily state or reflect those of the United States Government or any agency thereof or the Regents of the University of California.

UCRL-11947

UNIVERSITY OF CALIFORNIA

Lawrence Radiation Laboratory
Berkeley, California

AEC Contract No. W-7405-eng-48

(d,α) REACTIONS ON C^{12}, N^{14} AND O^{16} INDUCED BY 24 MeV DEUTERONS

Richard H. Pehl, Joseph Cerny, Ernest Rivet, and Bernard G. Harvey

May 1965

(d,α) REACTIONS ON C^{12}, N^{14} AND O^{16} INDUCED BY 24 MeV DEUTERONS*

Richard H. Pehl, Joseph Cerny, Ernest Rivet†, and Bernard G. Harvey

Lawrence Radiation Laboratory and Department of Chemistry
University of California
Berkeley, California

May 1965

ABSTRACT

Alpha-particle energy spectra from (d,α) reactions on C^{12}, N^{14} and O^{16} have been obtained using 24-MeV deuterons. The development of a high-resolution semiconductor E-dE/dx counter telescope made possible the observation of alpha-particle groups arising from the formation of final states of higher excitation than previously studied by these reactions. Angular distributions corresponding to resolvable final states are presented. Marked variation in the relative cross sections of final states was observed in the energy spectra. In an effort to explain the nature of this preferential population these final states are correlated, where possible, with their expected configurations. A DWBA analysis was made for several of the transitions; the outstanding characteristic of this analysis was the strong preference for L=2 transitions relative to L=0 transitions.

I. INTRODUCTION

The removal of two nucleons from the target nucleus in a direct reaction should favorably excite levels in the product nucleus whose configuration corresponds to two holes in the target. Thus, states not strongly excited in single-nucleon transfer reactions can be investigated. Although many (d,α) reactions in the light elements have been studied, most of them have involved either the use of single-counter systems or very low bombarding energies and consequently the observable excitation in the residual nucleus was severely limited. The development of a semiconductor counter telescope system[1] has enabled us to investigate the formation of states of higher excitation.

A measurement of the relative cross sections to the levels in a given nucleus made by different reactions—e.g., $C^{12}(\alpha,d)N^{14}$, $N^{14}(\alpha,\alpha')N^{14*}$, and $O^{16}(d,\alpha)N^{14}$—can give information concerning both the configuration of the levels and the reaction mechanisms involved. It should be emphasized that these two facets are inherently tied together. Several such comparisons are discussed in this work.

II. EXPERIMENTAL

These (d,α) reactions were induced by the 24-MeV deuteron beam of the late Crocker Laboratory 60-inch cyclotron. The beam was brought out through an iron magnetic channel, focused by a quadrupole magnet, and directed by a small steering magnet through a 4.8-mm diameter graphite collimator and a 4.8-mm diameter tantalum baffle collimator into a 91-cm diameter scattering chamber. The general experimental apparatus has been described previously.[2]

Particles were detected by a counter telescope that consisted of two semiconductor counters: a 2.7-mil phosphorous-diffused silicon transmission counter[1] backed by another phosphorous-diffused silicon counter,[3] which had a

depletion thickness of 67 mg/cm^2 when a 240-V reverse bias was applied. When studying reactions producing alpha particles having a range greater than 67 mg/cm^2 (23 MeV), lithium-drifted p-i-n junction silicon detectors[4] of various thicknesses were used. The counter telescope was placed from 20 to 32 cm from the target. The diameter of the collimator that preceded the transmission counter was usually 1.5 mm.

To compensate for the loss of resolution in the stopping counter due to the (nonuniform) transmission counter, the pulses from the two counters were added in the appropriate ratio. The optimum resolution of the added pulses was about 240 keV for solid targets, which was probably limited by the approximately 0.75% energy spread in the cyclotron beam. The simple passive pulse-adder circuit is shown in the block diagram of the counting equipment, Fig. 1.

The reaction products were distinguished by an analog pulse multiplier. A multiplier spectrum with optimum He^3-He^4 separation is shown in Fig. 2. Even though the transmission counter was very thin the low-energy alpha particles leaving a highly excited residual nucleus deposited a large fraction of their energy in the ΔE detector. However, the multiplier apparently worked properly (i.e., the multiplier output signal remained essentially constant) when as much as 95% of the alpha energy was dropped in the ΔE counter.

Generally the He^3-He^4 separation was not sufficiently good to permit complete removal of He^3 peaks from the alpha spectra without also discriminating against some alpha particles. Consequently multiplier pulses, corresponding to both He^3 and He^4 ions, were, in most cases, used to trigger a RIDL 400-channel pulse-height analyzer which recorded a single energy spectrum of both kinds of particles. However, several energy spectra were obtained when the lower discriminator corresponded to the center of the He^3-He^4 valley. This is discussed more thoroughly later.

Carbon targets about 0.3 mg/cm^2 thick were prepared as described previously.[5] Natural nitrogen and oxygen gases were bombarded in the gas-holder target assembly described previously.[6] The gas pressures ranged from 45- to 73-cm Hg at about 18°C.

III. RESULTS

A. The $C^{12}(d,\alpha)B^{10}$ Reaction

Previous investigations of this reaction have been carried out at bombarding energies up to 20 MeV.[7,8,9] Most of these studies were done with single-counter systems and consequently the observable excitation in B^{10} was usually restricted to about 5 MeV, and usually no levels above the 3.58-MeV level were resolved.

We have obtained alpha-particle energy spectra corresponding to an excitation in B^{10} up to about 12 MeV. The angular range studied covered from 6.3 to 71.4 deg (lab). Figures 3 and 4 show alpha-particle energy spectra at 45 and 16 deg, respectively. Table I presents a comparison of the B^{10} levels observed with those previously reported.

One of our reasons for investigating this reaction was to test isospin conservation at this energy. Many (d,α) isospin "forbidden" transitions have been previously investigated, but most of the specific transitions studied have been 0+, T=0 → 0+, T=1 reactions and for these transitions it is impossible to conserve angular momentum and parity, in addition to requiring nonconservation of isotopic spin.[2] Consequently, if one desires to test the isospin selection rule via the (d,α) reaction, transitions other than 0+, T=0 → 0+, T=1 must be studied.

The transitions to the 2+, T=1 and 3-, T=1 levels at 8.89-MeV excitation satisfy the above conditions and, furthermore, these levels are sufficiently

separated from any known T=0 levels that their peak in the alpha-particle energy spectra would be completely resolved if no complicating factors entered the picture. Unfortunately a peak arising from He^3 ions from the $C^{12}(d,He^3)B^{11}$ ground-state reaction falls in the region of interest on the energy spectra, as shown in Figs. 3 and 4. To remove this peak from the energy spectra the lower discriminator on the multiplier pulse was adjusted to correspond to the center of the He^3-He^4 valley. Figures 5 and 6 show the energy spectra obtained when the gates are adjusted for He^4 and He^3, respectively. Although the He^3-He^4 separation obtained with the multiplier was not sufficient to completely remove the He^3 peaks from the alpha-energy spectra without also losing a few alpha particles, it was good enough to make the He^3 peak a secondary problem. As Fig. 5 illustrates, an alpha-particle continuum arising from several-body breakup begins at a position in the energy spectra corresponding to an excitation of about 4.5 MeV. This continuum would obscure a level made with relatively small cross section at 8.89-MeV excitation. However, none of the energy spectra obtained when the He^3 ions were gated out show any indication of a peak rising above the continuum in the 8.89-MeV excitation region.

Precise analysis of the energy spectra above an excitation of about 6 MeV is severely hampered by the continuum, and no angular distributions were obtained for levels above the 6.04-MeV level. The angular distributions of the alpha particles corresponding to formation of the B^{10} ground state, 0.717-, 2.15-, 3.59-, 4.77-, 5.18-, and 6.04-MeV levels are presented in Figs. 7, 8, and 9. The error bars shown are typical and represent counting statistics only; the angular accuracy in all cases is about ±0.3 deg. Table II lists the integrated cross sections for the eight B^{10} levels analyzed.

Since the 4.77-MeV level is made with a large cross section in this and previous (d,α) investigations,[10,11] the doubtful isospin assignment[8] of T=0 is certainly correct. The levels at 6.04, 6.67, and 7.05 MeV also have T=0 since they are formed with a relatively large cross section in our work.

At no angle was an alpha particle group corresponding to formation of the 0+, T=1 level at 1.74-MeV level observed. The absence of this group is expected, as discussed earlier. An upper limit for this transition can be set at about 1% of the ground state cross section.

B. The $N^{14}(d,\alpha)C^{12}$ Reaction

Previous investigations of this reaction have been made at bombarding energies up to 21 MeV.[7,8] The large positive Q value (13.57 MeV) allows one to use a single counter and still observe fairly high excitation in C^{12}. Our investigation was accomplished primarily with a single counter since the study of this reaction was essentially completed before the thin transmission counters were developed. Energy spectra were obtained over the angular range from 10 to 130 deg. The observable excitation ($\theta < 50$ deg) reached about 13 MeV when the single counter was used, but as shown in Fig. 10, this range was extended to about 22 MeV for the spectra obtained using the multiplier. Peaks corresponding to He^3 ions from the $N^{14}(d,He^3)C^{13}$ reaction enter the spectra at C^{12} excitations greater than 15 MeV. A comparison of the C^{12} levels observed with those previously reported is presented in Table III. As Fig. 10 illustrates, an alpha particle continuum begins at a position in the energy spectra corresponding to an excitation of about 7.5 MeV.

The angular distributions of the alpha particles corresponding to formation of the C^{12} ground state, 4.43-, 7.66-, and 9.64-MeV levels are presented in Fig. 11. The error bars shown are typical and represent counting statistics only; the circles used to represent the 4.43-MeV level usually encompassed the statistical uncertainty. The uncertainty of the absolute values of the differential cross sections to the ground state and 4.43-MeV level was estimated to be less than 10%. However, the alpha particle continuum prevents such a precise

analysis of the 7.66- and 9.64-MeV levels. The integrated cross sections for the transitions to the ground state and 4.43-MeV level were 0.52 mb (13.0 to 137.6 deg c.m.) and 3.50 mb (13.1 to 138.1 deg c.m.), respectively. No angular distribution is presented for the 12.71-MeV level because it was not observed over a wide range of angles, and because the alpha continuum and the nearby He^3 ions make it very difficult to determine accurate values. However, the differential cross section to the 12.71-MeV level appears to be comparable to the 4.43-MeV level.

It is noteworthy that the two highly populated levels (4.43- and 12.71-MeV) are both mainly $(p_{3/2})^7(p_{1/2})^1$ configurations whereas the two 0+ levels (ground state and 7.66-MeV) are mixtures of the $(p_{3/2})^8$ and $(p_{3/2})^6(p_{1/2})^2$ configurations.[12] No statistical factor is included when comparing the cross sections of different levels made by a given pickup reaction since this factor

$$\frac{d\sigma}{d\Omega} \propto \frac{2I_f+1}{2I_i+1} ,$$

where I_i and I_f are the spins of the incident and outgoing particles, respectively, is independent of the spins of the initial and final nuclear levels.[13]

Formation of the 3- level at 9.64 MeV would require raising one p shell nucleon into a $d_{5/2}$ shell in addition to the removal of two nucleons. However, this level is observed, and in considerably larger yield than the 7.66-MeV level. Unless the N^{14} ground state contains an appreciable $d_{5/2}$ admixture this level must be formed primarily by a knockout mechanism if one assumes that these transitions, which involve relatively high incident and outgoing energies, go entirely by a direct process.

Table IV shows the approximate relative cross sections for several C^{12} levels made via the $B^{10}(\alpha,d)C^{12}$,[14] $C^{12}(\alpha,\alpha')C^{12*}$,[15] and $N^{14}(d,\alpha)C^{12}$ reactions, and their dominant configurations. For the (α,d) reaction the cross section to each level is divided by $(2J_f+1)$, relative to the ground state cross section

divided by $(2J_{g.s.}+1)$ to remove the statistical factor for stripping reactions. This is the only (d,α) reaction studied that strongly favors the population of excited states relative to the ground state transition.

C. The $O^{16}(d,\alpha)N^{14}$ Reaction

Previous investigations of this reaction have been carried out at bombarding energies up to 20 MeV,[7,8,9] but the observable excitation in N^{14} was usually restricted to 4 MeV at the most. In our work alpha-particle energy spectra corresponding to excitation in N^{14} up to about 13 MeV have been obtained. The angular range studied covered from 9.6 to 90 deg. Figures 12 and 13 show alpha-particle energy spectra at 22 and 61 deg, respectively.

The large broad peak that appears at an excitation between 11 and 12 MeV in Fig. 12 must be an alpha peak because all other possibilities can be eliminated. The first-excited state in N^{15} lies 5.28 MeV above the ground state; thus the observed peak cannot arise from a $O^{16}(d,He^3)N^{15*}$ transition. A large peak at about this excitation is also observed in the reaction $N^{14}(\alpha,\alpha')N^{14*}$.[16]

Observation of the levels at 8.47 and 9.41 MeV in this reaction indicates that these levels have T=0. Further evidence for the T=0 nature of these levels comes from a recent study of the $C^{12}(\alpha,d)N^{14}$ reaction.[5] Angular distributions of the alpha particles corresponding to formation of the N^{14} ground state, 3.95-, 4.91-, and 5.10-, 5.69-, and 5.83-, 6.21- and 6.44-, and 7.03-MeV levels are shown in Figs. 14 and 15. The three "doublets" were treated as a single peak since the experimental resolution was not sufficient to allow these levels to be

analyzed separately. Typical error bars, which represent counting statistics only, are shown. Table V presents the integrated cross sections for the N^{14} levels analyzed; the uncertainty of the absolute values of the differential cross sections was estimated to be less than 10%.

Extensive theoretical studies of the N^{14} nucleus have been made.[12,17,18] Consequently the observed selectivity in the formation of the N^{14} levels via different reactions is especially interesting. For example, N^{14} levels formed strongly in the reaction $O^{16}(d,\alpha)N^{14}$ should be those whose configurations are such that they can be produced by simple removal of two nucleons from O^{16} if the reaction proceeds by double pickup. One would not expect to form N^{14} levels in which one or more nucleons are in the $2s_{1/2}$ or $1d_{5/2}$ shells, since the amplitudes for such configurations are probably not large in O^{16}. The $C^{12}(\alpha,d)N^{14}$ reaction should populate the N^{14} levels whose configurations are an unchanged C^{12} core plus two nucleons, and the $N^{14}(\alpha,\alpha')N^{14*}$ reaction should show which N^{14} levels can be made by the excitation of a single nucleon. Table VI presents the relative cross sections for a number of N^{14} levels and their dominant configurations. For the (α,d) reaction the cross section of each level is divided by $(2J_f+1)$, relative to the ground state divided by $(2J_{g.s.}+1)$.

In general the (α,d) results are in excellent agreement with the shell-model assignments.[5] However, the (d,α) results are more difficult to understand. The double closed-shell configuration of O^{16} could, by removal of two nucleons, produce the levels at 0, 3.95, and 7.03 MeV. But formation of the levels at 4.91, 5.10, 5.69, and 5.83 MeV would require raising one p-nucleon into an s or d shell in addition to the removal of two nucleons, and formation of the levels at 6.21 and 6.44 MeV would require raising two p nucleons into the s and/or d shell. These last six levels were observed, although in slightly reduced yield. All these levels could arise from an admixture of $[p^{-2}(s_{1/2})^2 + p^{-2}(s_{1/2}d_{5/2}) + p^{-2}(d_{5/2})^2]$ in the O^{16} ground state. These levels could also be

formed by a) a compound nucleus mechanism; b) knockout of an alpha particle from the $(p_{3/2})^8$ $(p_{1/2})^4$ configuration and capture of one or both nucleons of the incident deuteron in the s or d shells. To eliminate compound nucleus formation, this reaction could be studied at higher energies to see if the (sd) states are still strongly populated.

Additional information on the nature of the N^{14} levels and/or the configuration of the O^{16} ground state is provided by the analogous two-nucleon pickup reactions, $O^{16}(p,He^3)N^{14}$ and $O^{16}(He^4,Li^6)N^{14}$. Figures 16 and 17 show energy spectra we have recently obtained from these reactions, using 43.7-MeV protons and 80.6-MeV alpha particles, respectively. From the $O^{16}(p,He^3)N^{14}$ spectrum it can be seen that states at 0, 2.31, 3.95, 7.03, and about 9.15 MeV are strongly populated. These states are the only ones of configuration $1p^{10}$ through 9.4 MeV excitation, and none of the (sd) states are populated to an appreciable fraction of the p^{10} states. Thus the spectroscopy of the final states observed in the (p,He^3) reaction supports a simple pickup mechanism and negligible (sd) admixture in the O^{16} ground state.

On the other hand, the $O^{16}(He^4,Li^6)N^{14}$ spectra appear more similar to the (d,α) results. The (sd) states are populated fairly strongly, especially at larger angles. Consequently, assuming a specific O^{16} ground state configuration, one could arrive at very different conclusions regarding the reaction mechanism depending upon which of these three supposedly analogous two-nucleon transfer reactions he studied (ignoring expected differences in population of T=1 final states).

IV. DISCUSSION

A. Pseudo Detailed Balance

Time reversal invariance implies a detailed balance between nuclear reactions, although the inverse statement is not always true.[20] If a detailed balance is to be observed in the reactions

$$A + 2 + d \rightleftarrows A + \alpha$$

the bombarding energies must be adjusted so that the excitation of the compound system is the same in both directions. However, for a simple plane-wave treatment the energy dependence of the differential cross section enters only through the momentum transfer. For a given momentum transfer the differential cross sections are related by

$$\left(\frac{d\sigma}{d\Omega}\right)_{d,\alpha} = \frac{(2J_\alpha+1)(2J_A+1)}{(2J_d+1)(2J_{A+2}+1)} \left(\frac{p_\alpha}{p_d}\right)_{d,\alpha} \left(\frac{p_\alpha}{p_d}\right)_{\alpha,d} \left(\frac{d\sigma}{d\Omega}\right)_{\alpha,d} .$$

Thus a pseudo detailed balance can be made by varying the angles at which the differential cross sections are to be compared so that the momentum transfer of the two reactions is equal. Similar comparisons were first made by Legg.[21]

Figure 18 shows a comparison of the angular distributions obtained with 23.8-MeV deuterons $[O^{16}(d,\alpha)N^{14}]$ and 46.5-[6] and 42-MeV[14] alpha particles $[N^{14}(\alpha,d)O^{16}]$. The corresponding compound system excitations are 28.6, 40.5, and 37.1 MeV, respectively, so that the energy matching conditions are far from satisfied. For this comparison, and for the comparisons illustrated later, the momentum transfer was calculated on the basis of pickup and stripping kinematics for the (d,α) and (α,d) reactions, respectively. The magnitudes of the (α,d) cross sections were multiplied by the factors needed to satisfy the above equation.

Figure 19 shows a comparison of the $N^{14}+d \rightleftarrows C^{12}+\alpha$ angular distributions obtained with 23.8-MeV deuterons and 48-MeV alpha particles.[2] These relative energies are almost appropriate for a detailed balance with compound-system excitations of 41.7 and 43.1 MeV, respectively. Consequently Fig. 19 compares the cross sections directly without adjusting to get exact momentum-transfer equality. The shift needed to obtain exact equality is about 1.5 deg in the direction of better agreement.

A comparison of the $C^{12}+d \rightleftarrows B^{10}+\alpha$ angular distributions obtained with 24.1-MeV deuterons and 42-MeV alpha particles[14] is shown in Fig. 20. With compound-system excitations of 31.0 and 41.6 MeV the energy matching conditions are far from being satisfied.

The $N^{14}+d \rightleftarrows C^{12}+\alpha$ system definitely exhibited the best agreement, as expected since it came nearest to satisfying the relative energy requirements. However, all the comparisons showed fairly good agreement, especially at small angles, which suggests that a plane-wave treatment has some merit for those transitions. This agreement also indicates that the absolute values of the (d,α) cross sections are probably quite accurate.

B. Distorted-Wave Calculations

The general form of the differential cross section for two-nucleon transfer reactions has been derived and discussed extensively by Glendenning[13] and consequently will not be repeated here. An optical-model program written by Dr. N. K. Glendenning was used for the optical-model analysis. Only a summary of this analysis will be presented here (Ref. 22 contains a more complete discussion). The parameters used are listed in Table VII and typical fits are shown in Figs. 21 and 22. Many of the "fits" obtained could undoubtedly be improved if a more extensive analysis were undertaken. It was felt, however, that such an analysis was not

warranted at the present time because of the amount of computer time that would be required, with little to gain as far as the calculation of (d,α) angular distributions was concerned.

The DWBA calculations were made with another program written by Glendenning. These calculations are based on the approximations that the reaction occurs only at a specific radius (this position is commonly called the surface), and that the two nucleons are picked up as a lump, i.e., reference to the single-particle orbits from which the nucleons are picked up is suppressed. Therefore, the reaction is characterized by the total angular momentum L that is transferred and this is the only information that can be obtained from fitting the angular distributions with this simple code.

Calculations were made at a series of interaction radii to determine what radius gave the best fit. The optical-model parameters were then varied to see if a better fit could be obtained. In no case was an improved fit found. Since the calculation did not give the absolute magnitude of the cross section, the fits shown involve an arbitrary normalization.

The specific fits are now discussed individually. The allowed L values for the $N^{14}(d,\alpha)C^{12*}$(4.43-MeV) transition are 0, 2, and 4. However, if p-shell nucleons are being picked up, L=4 is not allowed since two p nucleons can couple to a maximum of L=2. Since the calculation is performed without reference to the shells from which the nucleons are picked up, L=4 is included as a possibility with the hope that L=4 will give an inferior fit. Figure 23 shows the best fit obtained. Although different relative intensities of the allowed L transfers were tried, the best fit corresponded to nearly 100% L=2. No combination of different interaction radii and/or optical-model parameters that were tried gave any indication that a better fit could be obtained by using an admixture of L=0 and/or L=4. Of course, small admixtures, up to about 10%, could be included without definitely producing an inferior fit. However, the fit presented is for pure L=2.

The allowed L values for the $N^{14}(d,\alpha)C^{12}$ ground state transition are 0 and 2, and once again the best fit corresponds to almost 100% L=2 (see Fig. 24). As in the above case and for all the other transitions analyzed, no combination of different interaction radii and/or optical-model parameters that was tried gave any indication that a better fit could be obtained by using an appreciable admixture of $L \neq 2$. Fits to the $O^{16}(d,\alpha)N^{14}$ and $C^{12}(d,\alpha)B^{10}$ ground state transitions, shown in Figs. 25 and 26, also show a strong preference for L=2.

The outstanding feature of these calculations is that L=2 transitions are strongly enhanced over L=0 transitions. This is not surprising if the reaction takes place primarily at the surface, because only partial waves in the entrance and exit channels in the vicinity of $L_d = k_d R$ and $L_\alpha = k_\alpha R$, respectively, will be expected to contribute strongly. Since the angular momentum transferred to the core is given by

$$\vec{L} = \frac{M_f}{M_i} \vec{L}_d - \vec{L}_\alpha$$

the reaction will be inhibited when this equality is not satisfied. Calculations of $\vec{L}$ over the appropriate angular region for all the transitions analyzed give values greater than 2, and thus L=2 transitions would be expected to be favored, compared with L=0 transitions. Furthermore, the momentum transfer for these (d,α) reactions does not change appreciably as a function of bombarding energy, and thus L=2 should be favored at all bombarding energies.

The enhancement of L=2 over L=0 transitions is also in accord with predictions based on the coupling scheme used by Glendenning[25] for two-nucleon transfer reactions. The nuclear structure factors arising in this model for (d,α) reactions permit only ^3S configurations for the picked-up nucleons when the initial and final states are described in pure j-j coupling. The results from these calculations indicate that L=2 transitions would be strongly enhanced even

Improvements in the art of making distorted-wave calculations will undoubtedly allow one to garner more information from fitting angular distributions than was possible with the relatively simple program used here. At present, however, the study of two-nucleon transfer angular distributions does not appear to be as valuable a spectroscopic tool as the investigation of the preferential population of final states.

ACKNOWLEDGMENTS

We wish to thank the crew of the Crocker Laboratory cyclotron for their efficient operation of the machine and their assistance with the experiments. It is a pleasure to thank J. H. Elliott and W. L. Hansen for developing the silicon detectors, N. K. Glendenning for use of his optical-model and two-nucleon transfer reaction programs, and B. D. Wilkins for assistance with the optical-model analysis.

REFERENCES

*This work was done under the auspices of the U. S. Atomic Energy Commission.

†Present address: University of Montreal, Montreal, Quebec

1. J. H. Elliott and R. H. Pehl, Rev. Sci. Instr. 33, 713 (1962).
2. B. G. Harvey and J. Cerny, Phys. Rev. 120, 2162 (1960).
3. These counters were developed by W. L. Hansen, Lawrence Radiation Laboratory, Berkeley, California.
4. J. H. Elliott, Nucl. Instr. Methods 12, 60 (1961).
5. R. H. Pehl, E. Rivet, J. Cerny, and B. G. Harvey, Phys. Rev. 137 B114 (1965).
6. J. Cerny, B. G. Harvey, and R. H. Pehl, Nucl. Phys. 29, 120 (1962).
7. F. Ajzenberg-Selove and T. Lauritsen, Nucl. Phys. 11, 1 (1959).
8. T. Lauritsen and F. Ajzenberg-Selove, Nuclear Data Sheets, NRC 61-5,6, (National Academy of Sciences-National Research Council, Washington, 1962).
9. T. Yanabu, S. Yamashita, T. Nakamura, K. Takamatsu, A. Masaike, S. Kakigi, D. C. Nguyen, and K. Takimoto, J. Phys. Soc. Japan 18, 747 (1963).
10. F. Pellegrini, Nucl. Phys. 24, 372 (1961).
11. J. Catalá, A. Bonet, and E. Villar, Anales Real Soc. Espan. Fis. Quim (Madrid) A54, 241 (1958).
12. I. Talmi and I. Unna, Annual Review of Nuclear Science, Vol. 10 (Annual Reviews, Inc., Palo Alto, Calif., 1960), p. 353.
13. N. K. Glendenning, Annual Review of Nuclear Science, Vol. 13 (Annual Reviews, Inc., Palo Alto, Calif., 1963), p. 191; Phys. Rev. 137, B 102 (1965).
14. C. D. Zafiratos, (Ph.D. Thesis) University of Washington, Seattle, May 1962 (unpublished).
15. F. J. Vaughn, (Ph.D. Thesis), University of California Radiation Laboratory Report UCRL-3174, 1955 (unpublished).
16. B. G. Harvey, J. Cerny, R. H. Pehl, and E. Rivet, Nucl. Phys. 39, 160 (1962).

17. E. K. Warburton and W. T. Pinkston, Phys. Rev. 118, 733 (1960).

18. W. W. True, Phys. Rev. 130, 1530 (1963).

19. E. Kashy, R. R. Perry, R. L. Steele, and J. R. Risser, Phys. Rev. 122, 884 (1961).

20. E. M. Henley and B. A. Jacobsohn, Phys. Rev. 108, 502 (1957); 113, 225 (1959).

21. J. C. Legg, Phys. Rev. 129, 272 (1963).

22. R. H. Pehl, (Ph.D. Thesis), Lawrence Radiation Laboratory Report UCRL-10993, 1963 (unpublished).

23. G. E. Fischer and V. K. Fischer, Phys. Rev. 114, 533 (1959).

24. J. Aguilar, W. E. Burcham, J. Catalá, J. B. A. England, J. S. C. McKee, and J. Rotblat, Proc. Roy. Soc. (London) A254, 395 (1960).

25. N. K. Glendenning, Nucl. Phys. 29, 109 (1962).

Table I. Comparison of B^{10} levels observed in this experiment with those previously reported.[a]

Levels identified (MeV)	Previously reported levels		
	Energy (MeV)	J^{π}	T
0	0	3+	0
0.72 ± 0.02	0.717	1+	0
	1.74	0+	1
2.15 ± 0.02	2.15	1+	0
3.59 ± 0.02	3.59	2+	0
4.77 ± 0.03	4.77	(2+)	(0)
	5.11	(2-)	(0)
	5.16	(2+)	(1)
5.17 ± 0.05	5.18	$1^{(+)}$	0
	(5.37)		
	5.58		
	5.92	2+	
6.04 ± 0.05	6.04	4+	
	6.16		
?	6.42		
6.67 ± 0.11	6.57		
	(6.77)		
?	6.88		
7.05 ± 0.10	6.97		
?	(7.19)		
	7.47	2+	
	7.48	2-	1
	7.56	0+	(1)
	7.78	2-	
	(8.07)		
	(8.66)		
	8.89	2+	1
	8.89	(3-)	(1)
	9.7		(1)
	10.7		(1)

[a]References 7 and 8.

Table II. Integrated cross sections for B^{10}.

Level (MeV)	Cross section (mb)	Range of integration (in deg., c.m.)
0	4.8 ± 0.3	0 - 86
0.717	1.7 ± 0.2	9.4 - 86.4
2.15	1.2 ± 0.2	9.5 - 87
3.59	1.3 ± 0.2	9.6 - 87.7
4.77	1.5 ± 0.3	9.7 - 76.7
5.17	1.0 ± 0.4	9.8 - 77
6.04	2.2 ± 0.5	9.9 - 77.5

Table III. Comparison of C^{12} levels observed in this experiment with those previously reported.[a]

Levels identified (MeV)	Previously reported levels		
	Energy (MeV)	J^{π}	T
0	0	0+	0
4.43 ± 0.03	4.433	2+	0
7.66 ± 0.05	7.656	0+	0
9.64 ± 0.05	9.64	3-	0
	10.1	(0+)	0
	10.84	(1-)	
	11.83	(1-)	
12.71 ± 0.07	12.71	(1+)	0
	13.34		

[a]References 7 and 8.

Table IV. Shell-model configurations and relative cross sections for the formation of C^{12} levels.

Level MeV	J^{π}	T	Dominant configuration[a]	Relative cross sections (α,d)	(α,α')	(d,α)
0	0+,	0	$(p_{3/2})^8$ and $(p_{3/2})^6(p_{1/2})^2$	1	--	1
4.433	2+,	0	$(p_{3/2})^7(p_{1/2})^1$	0.3	1	7
7.656	0+,	0	$(p_{3/2})^8$ and $(p_{3/2})^6(p_{1/2})^2$	0.1	0.025	0.3
9.64	3-,	0	$(p_{3/2})^7(d_{5/2})^1$	0.2	0.5	0.8

[a]Reference 12.

Table V. Integrated cross sections for N^{14}.

Level (MeV)	Cross section (mb)	Range of integration (in deg., c.m.)
0	1.97	11.3 - 100.2
3.95	3.16	11.5 - 101.2
4.91 5.10	1.29	11.5 - 82.2
5.69 5.83	1.68	11.6 - 82.5
6.21 6.44	1.28	11.6 - 82.6
7.03	2.11	11.6 - 82.9

Table VI. Shell-model configurations and relative cross sections for formation of N^{14} levels.

Level MeV	J^{π}	T	Dominant configuration[a]	Relative cross sections (α,d)[b]	(α,α')[c]	(d,α)
0	1+	0	$(p_{1/2})^2$	1	--	1
2.31	0+	1	$(p_{1/2})^2$	e	e	e
3.95	1+	0	$(p_{3/2})^{-1}(p_{1/2})^{-1}$	0.3	strong	1.60
4.91	0-	0	$p_{1/2}s_{1/2}$	0.8[d]	strong	0.72
5.10	2-	0	$p_{1/2}d_{5/2}$			
5.69	1-	0	$p_{1/2}s_{1/2}$	0.5[d]	strong	0.94
5.83	3-	0	$p_{1/2}d_{5/2}$			
6.05			?	e	e	e
6.21	1+	0	$(s_{1/2})^2$	0.5[d]	very weak	0.72
6.44	3+	0	$s_{1/2}d_{5/2}$			
7.03	2+	0	$(p_{3/2})^{-1}(p_{1/2})^{-1}$	0.2	strong	1.19
7.40			?	e	e	e
7.60			?	e	e	e
7.97	2-	0	$p_{1/2}d_{3/2}$	0.2	weak	weak
8.06	1-	1	$p_{1/2}s_{1/2}$	e	e	e
8.47		0	?	f	weak	fairly strong[g]
8.63	0+	1	$(s_{1/2})^2$	e	e	e
8.71	0-	1	$p_{1/2}s_{1/2}$	e	e	e
8.91	3-	1	$p_{1/2}d_{5/2}$	e	e	e
8.99	1+	(0)	?	?	e	e
9.00	5+	0	$(d_{5/2})^2$	1.6	e	e
9.17	2+	1	$(s,d)+(p_{3/2})^{-1}(p_{1/2})^{-1}$	e	e	e
9.41	1-		$p_{1/2}d_{3/2}$ (?)	0.8	weak	fairly strong
9.51	2-	1	$p_{1/2}d_{5/2}$	e	h	e
9.71	1+		$(d_{5/2})^2$	0.4	h	very weak
10.09	1+	0	$s_{1/2}d_{5/2}$[i]	0.5	e	weak
10.22	1-		?	e	e	weak
10.42	2+	1	$s_{1/2}d_{5/2}$	e	e	e

[a]References 12, 17, 18.

[b]Reference 5.

[c]Reference 16.

[d]Assuming equal population of each magnetic substate of the unresolved pair of levels.

[e]Not observed.

[f]If spin is 1, this value is 1.1, if spin is 2, the values is 0.7.

[g]Obscured somewhat by He^3 peak.

[h]Obscured by He^3 peak arising from the $N^{14}(\alpha,He^3)N^{15}$ ground state transition.

[i]The assigned configuration is wrong if the spin of this level is 1+ as recently reported, instead of 2+ as previously thought.[19]

Table VII. Optical-model parameters used for fits illustrated.[a]

Reaction	Bombarding energy (MeV)	r_0	-V (MeV)	-W (MeV)	a (F)	b (F)	r_1 (F)	σ_R (mb)
$C^{12} + d$	28	1.20	59.26	12.92	0.617	0.60	0.75	865
$N^{14} + d$	20.9	1.20	54.18	11.73	0.612	0.65	0.75	970
$N^{14} + d$	27	1.20	54.62	10.0	0.716	0.70	0.75	926
$O^{16} + d$	26.3	1.20	55.90	12.64	0.655	0.55	0.75	955
$C^{12} + \alpha$	21.2	1.30	60.0	6.0	0.40	0.65	1.20	892
$C^{12} + \alpha$	38.1	1.30	32.64	9.00	0.474	0.60	1.20	893
$N^{14} + \alpha$	25.7	1.30	35.23	7.12	0.435	0.60	1.20	923

[a]Volume absorption is used for all sets; $r_W = r_0$.

Figure Captions

Fig. 1. The passive pulse-adder circuit, shown with complete electronics block diagram.

Fig. 2. Multiplier spectrum at a scattering angle of 15 deg from bombardment of O^{16} with 24-MeV deuterons.

Fig. 3. Alpha particle energy spectrum from the $C^{12}(d,\alpha)B^{10}$ reaction.

Fig. 4. Alpha particle energy spectrum from the $C^{12}(d,\alpha)B^{10}$ reaction.

Fig. 5. Alpha particle energy spectrum from the $C^{12}(d,\alpha)B^{10}$ reaction.

Fig. 6. He^3 energy spectrum from the $C^{12}(d,He^3)B^{11}$ reaction.

Fig. 7. Angular distributions of alpha particles from formation of the ground state, 0.72-, and 4.77-MeV levels of B^{10}.

Fig. 8. Angular distributions of alpha particles from formation of the 3.59- and 6.04-MeV levels of B^{10}.

Fig. 9. Angular distributions of alpha particles from formation of the 2.15- and 5.18-MeV levels of B^{10}.

Fig. 10. Alpha particle energy spectrum from the $N^{14}(d,\alpha)C^{12}$ reaction.

Fig. 11. Angular distributions of alpha particles from formation of the ground state, 4.43-, 7.66-, and 9.64-MeV levels of C^{12}.

Fig. 12. Alpha particle energy spectrum from the $O^{16}(d,\alpha)N^{14}$ reaction.

Fig. 13. Alpha particle energy spectrum from the $O^{16}(d,\alpha)N^{14}$ reaction.

Fig. 14. Angular distributions of alpha particles from formation of the ground state, 4.91- and 5.10-, 5.69- and 5.83-, and 6.21- and 6.44-MeV levels of N^{14}.

Fig. 15. Angular distributions of alpha particles from formation of the 3.95- and 7.03-MeV levels of N^{14}.

Fig. 16. He^3 energy spectrum from the $O^{16}(p,He^3)N^{14}$ reaction.

Fig. 17. Li^6 energy spectrum from the $O^{16}(He^4,Li^6)N^{14}$ reaction.

Fig. 18. Comparison of angular distributions of deuterons and alpha particles from the $O^{16} + d \rightleftarrows N^{14} + \alpha$ system.

Fig. 19. Comparison of angular distributions of deuterons and alpha particles from the $N^{14} + d \rightleftarrows C^{12} + \alpha$ system.

Fig. 20. Comparison of angular distributions of deuterons and alpha particles from the $C^{12} + d \rightleftarrows B^{10} + \alpha$ system.

Fig. 21. A plot of σ/σ_{Ruth} for 20.9-MeV deuterons scattered from N^{14}.[23] The solid line is the predicted value of σ/σ_{Ruth} obtained using the optical-model parameters listed in Table VII.

Fig. 22. A plot of σ/σ_{Ruth} for 38.1-MeV alpha particles scattered from C^{12}.[24] The solid line is the predicted value of σ/σ_{Ruth} obtained using the optical-model parameters listed in Table VII.

Fig. 23. Angular distribution of alpha particles from the $N^{14}(d,\alpha)C^{12*}$ (4.43-MeV) transition. The solid line was calculated for L=2, interaction radius = 5.25F, and the following optical-model parameters:

	V	W	a	b	r_0	r_1
deuteron	-55	-11	0.65	0.65	1.20	0.75
alpha	-33	- 9	0.47	0.60	1.30	1.20

Fig. 24. Angular distribution of alpha particles from the $N^{14}(d,\alpha)C^{12}$ ground state transition. The solid line was calculated for L=2, interaction radius = 5.25F, and the same optical-model parameters as in Fig. 21.

Fig. 25. Angular distribution of alpha particles from the $O^{16}(d,\alpha)N^{14}$ ground state transition. The solid line was calculated for L=2, interaction radius = 6.00F, and the following optical-model parameters:

	V	W	a	b	r_0	r_1
deuteron	-56	-12	0.65	0.55	1.20	0.75
alpha	-35	- 7	0.45	0.60	1.30	1.20

Fig. 26. Angular distribution of alpha particles from the $C^{12}(d,\alpha)B^{10}$ ground state transition. The solid line was calculated for L=2, interaction radius = 4.80F, and the following optical-model parameters:

	V	W	a	b	r_0	r_1
deuteron	-59	-13	0.60	0.60	1.20	0.75
alpha	-60	- 6	0.40	0.65	1.30	1.20

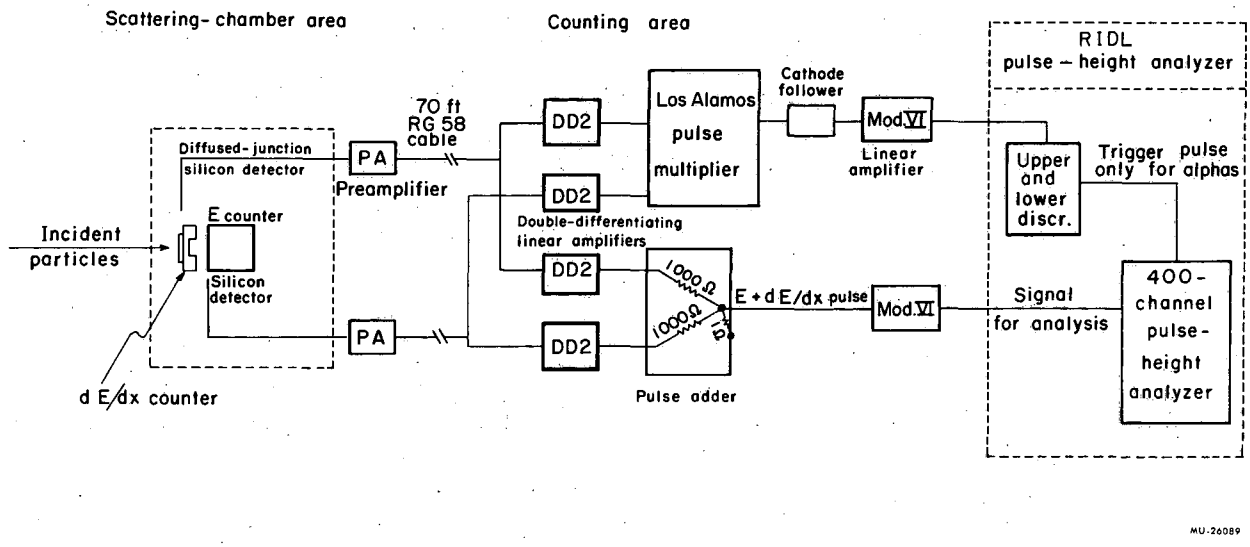
Scattering- chamber area
Counting area
RIDL
pulse – height analyzer
Diffused- junction
silicon detector
E counter
Silicon
detector
Incident
particles
d E/dx counter
PA
Preamplifier
70 ft
RG 58
cable
PA
DD2
DD2
DD2
DD2
Double-differentiating
linear amplifiers
Los Alamos
pulse
multiplier
Cathode
follower
1000 Ω
1000 Ω
1 Ω
Pulse adder
E + d E/dx pulse
Mod. VI
Linear
amplifier
Mod. VI
Upper
and
lower
discr.
Trigger pulse
only for alphas
Signal
for analysis
400-
channel
pulse-
height
analyzer
MU-26089

Fig. 1

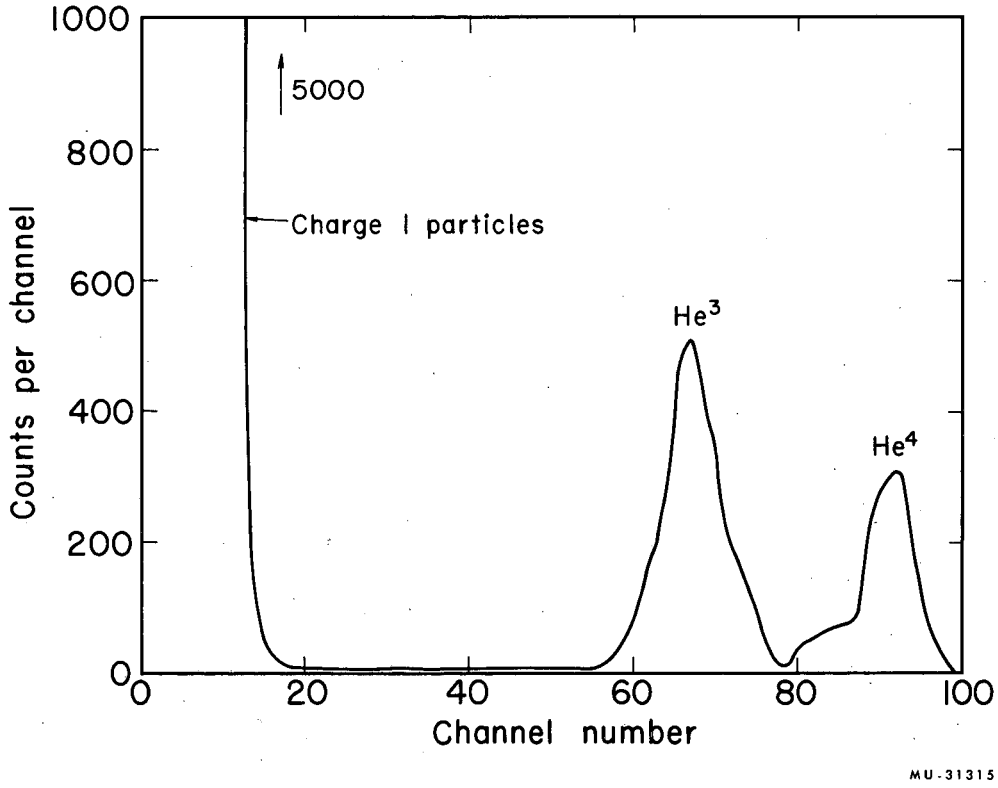
1000
800
600
400
200
0
Counts per channel
5000
Charge 1 particles
He3
He4
0
20
40
60
80
100
Channel number
MU-31315

Fig. 2

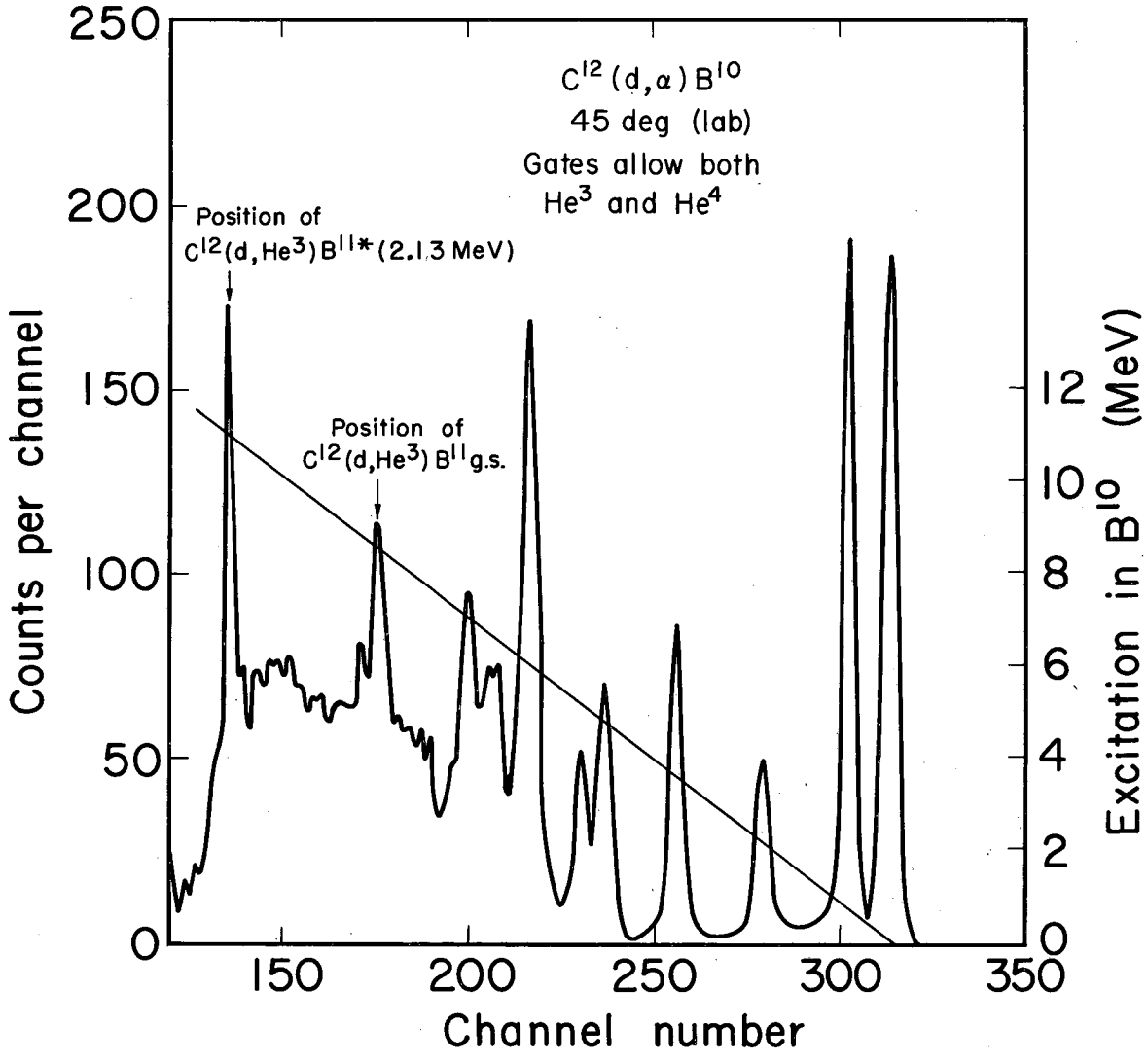

MUB-2126

Fig. 3

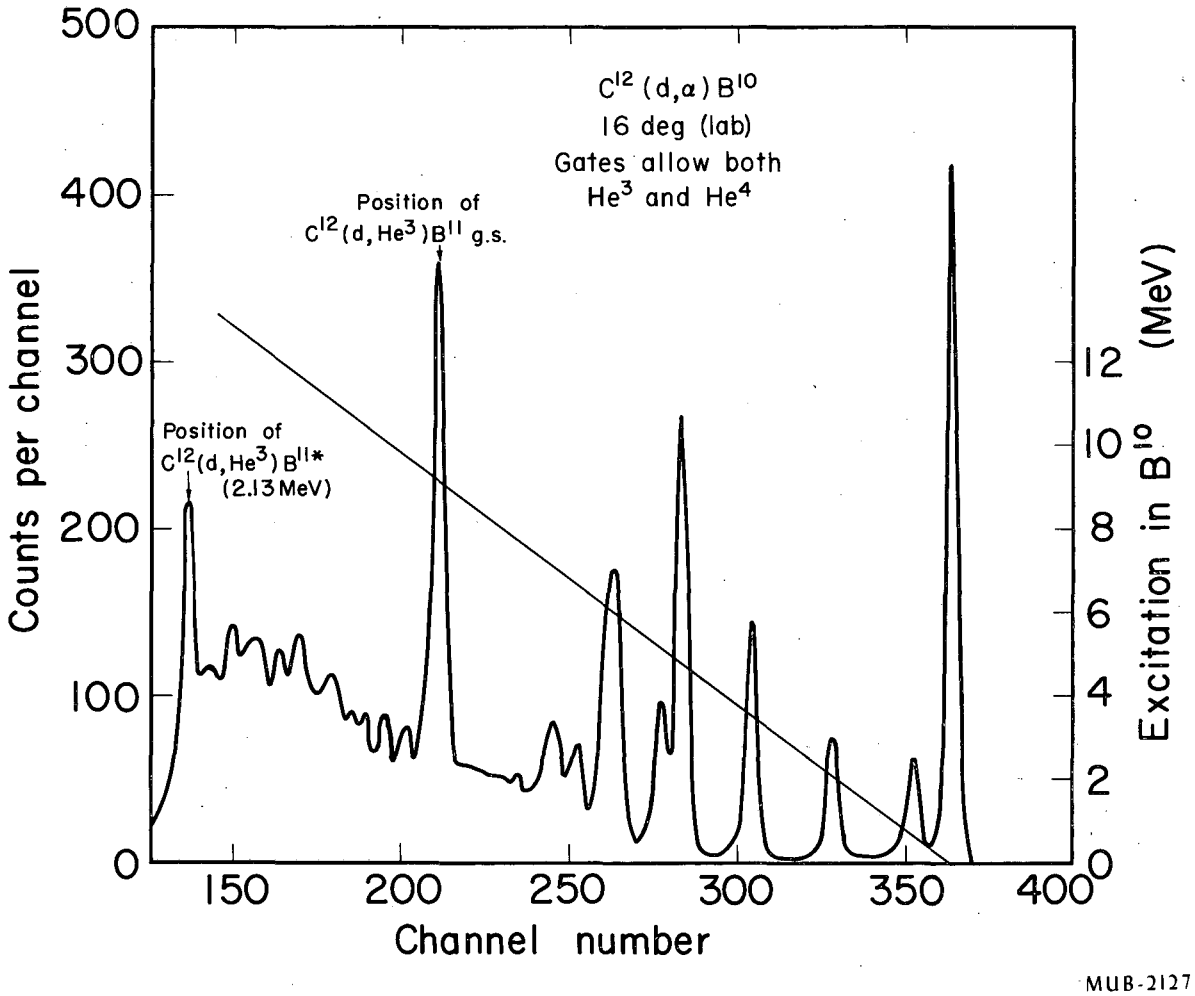

MUB-2127

Fig. 4

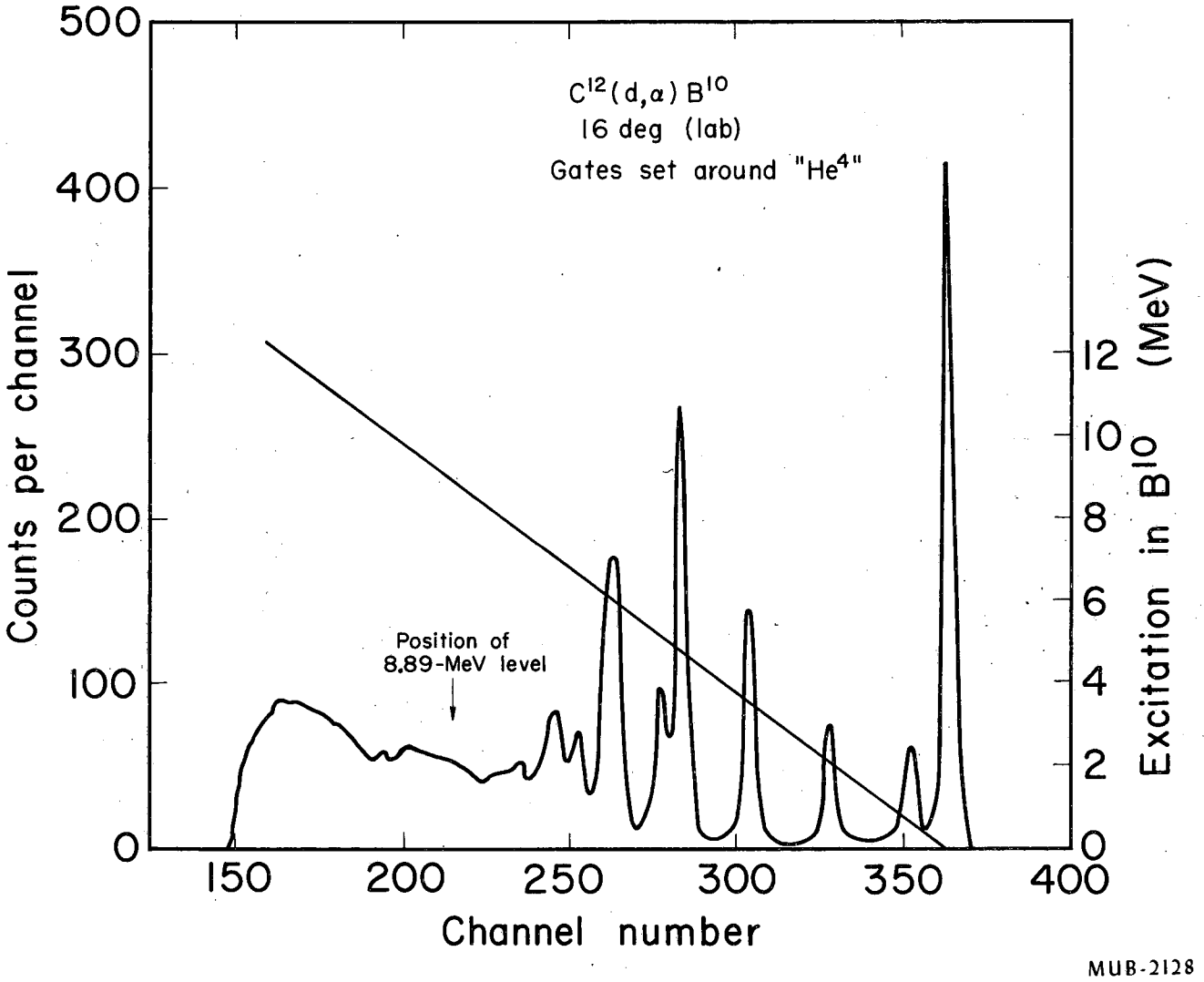
$C^{12}(d,\alpha)B^{10}$
16 deg (lab)
Gates set around "He^4"
Position of
8.89-MeV level
Counts per channel
Channel number
Excitation in B^{10} (MeV)
500
400
300
200
100
0
150
200
250
300
350
400
12
10
8
6
4
2
0
MUB-2128

Fig. 5

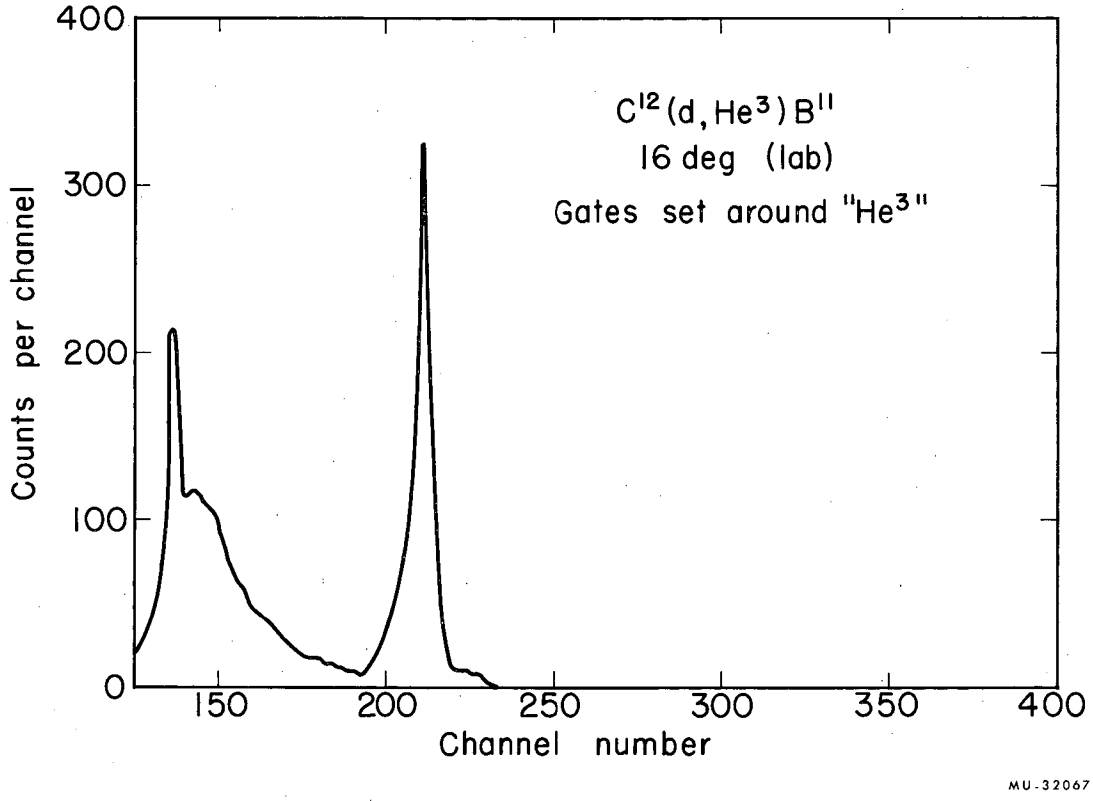
400
300
200
100
0
Counts per channel
150
200
250
300
350
400
Channel number
$C^{12}(d, He^3)B^{11}$
16 deg (lab)
Gates set around "He^3"
MU-32067

Fig. 6

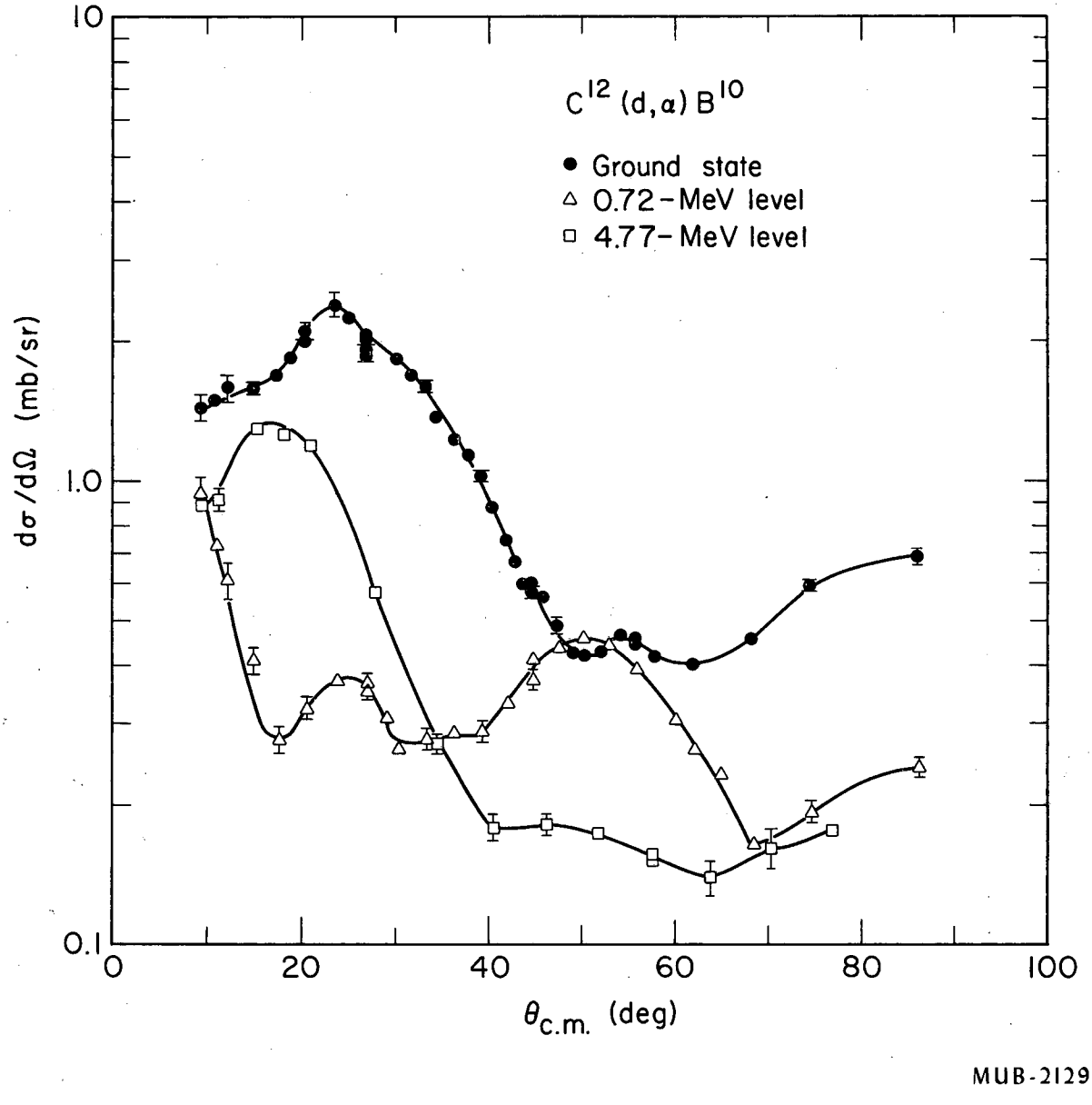

MUB-2129

Fig. 7

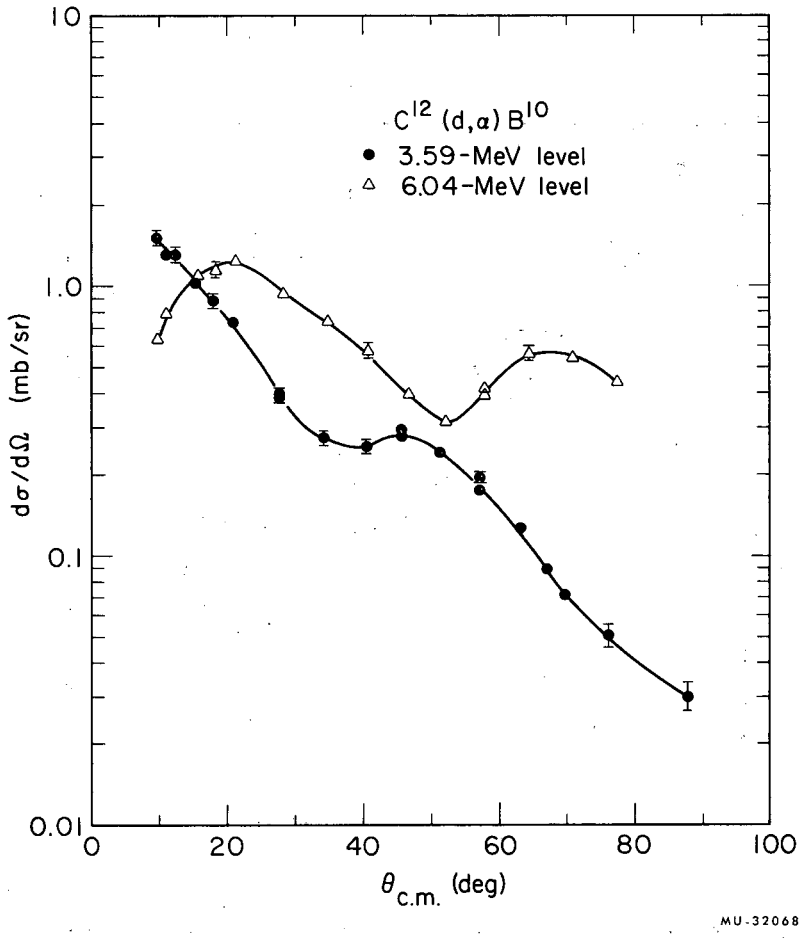
$C^{12}(d,\alpha)B^{10}$
3.59-MeV level
6.04-MeV level
10
1.0
0.1
0.01
$d\sigma/d\Omega$ (mb/sr)
0
20
40
60
80
100
$\theta_{c.m.}$ (deg)
MU-32068

Fig. 8

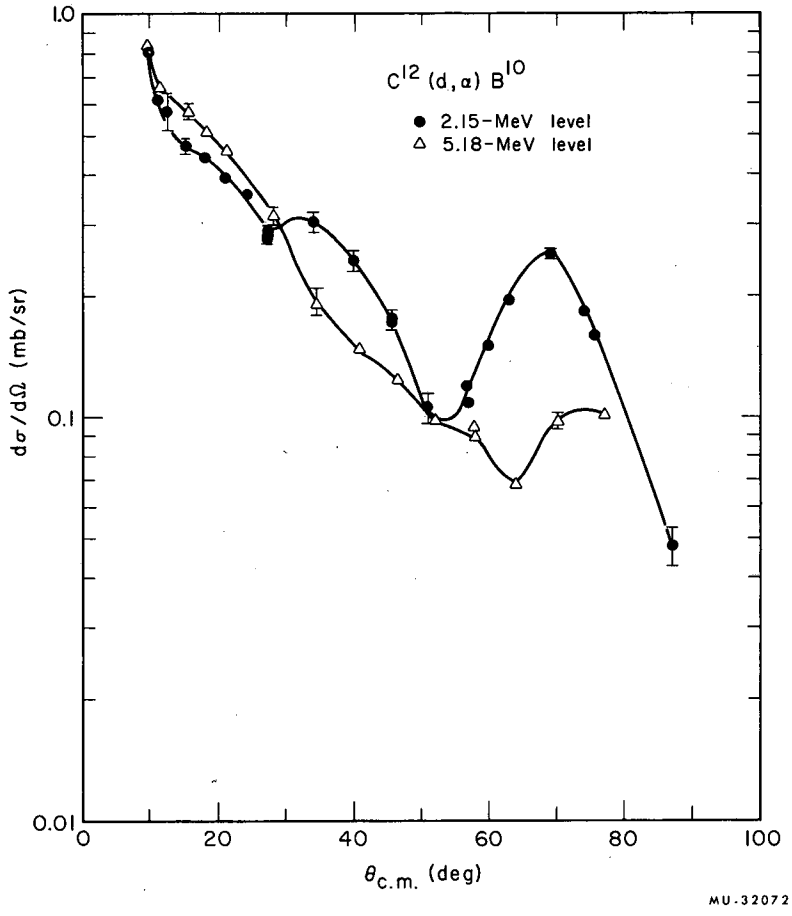
$C^{12}(d,\alpha)B^{10}$
● 2.15-MeV level
△ 5.18-MeV level
1.0
0.1
0.01
$d\sigma/d\Omega$ (mb/sr)
0
20
40
60
80
100
$\theta_{c.m.}$ (deg)
MU-32072

Fig. 9

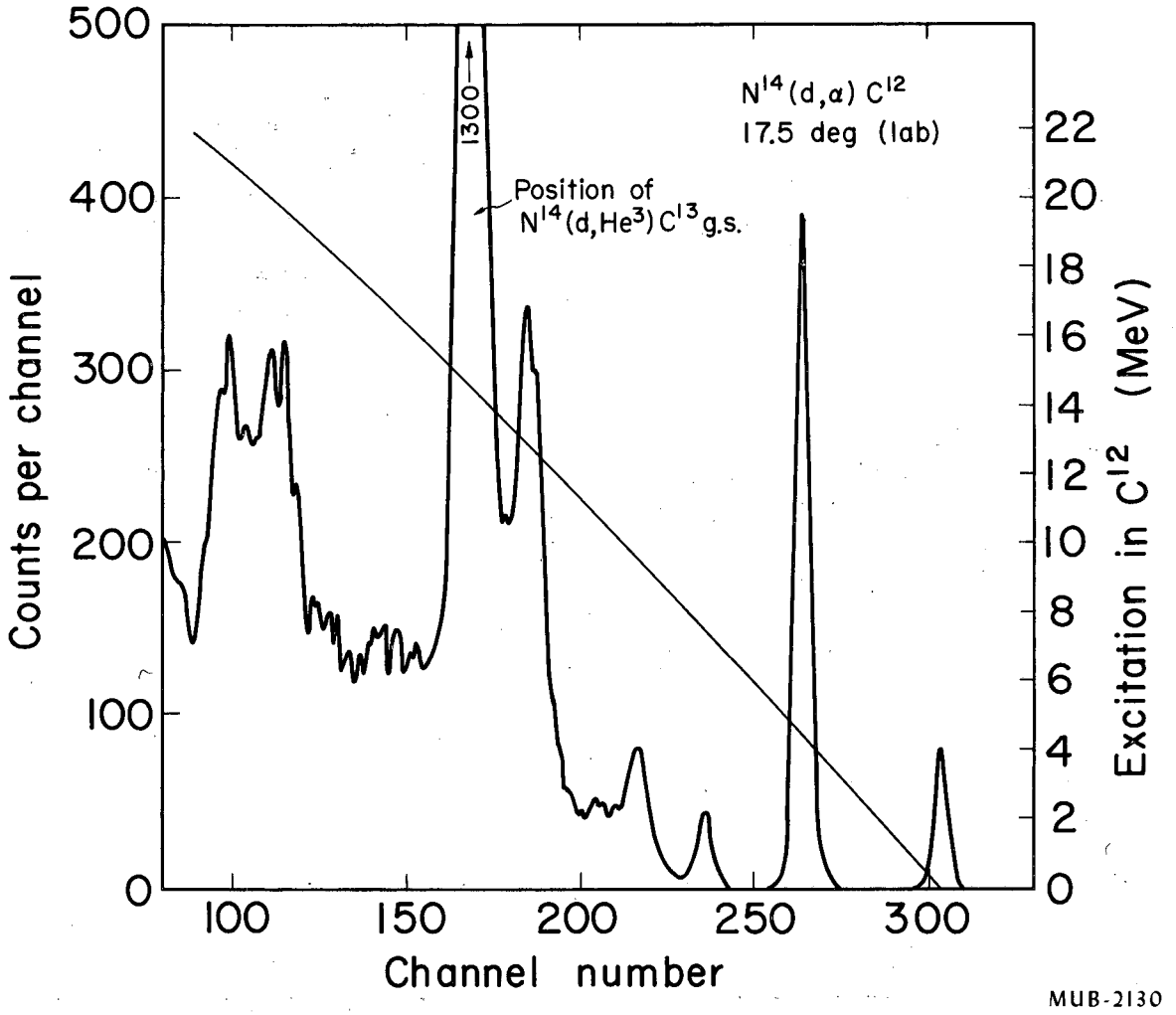
500
400
300
200
100
0
Counts per channel
1300
Position of
N14(d,He3)C13 g.s.
N14(d,α) C12
17.5 deg (lab)
22
20
18
16
14
12
10
8
6
4
2
0
Excitation in C12 (MeV)
100
150
200
250
300
Channel number
MUB-2130

Fig. 10

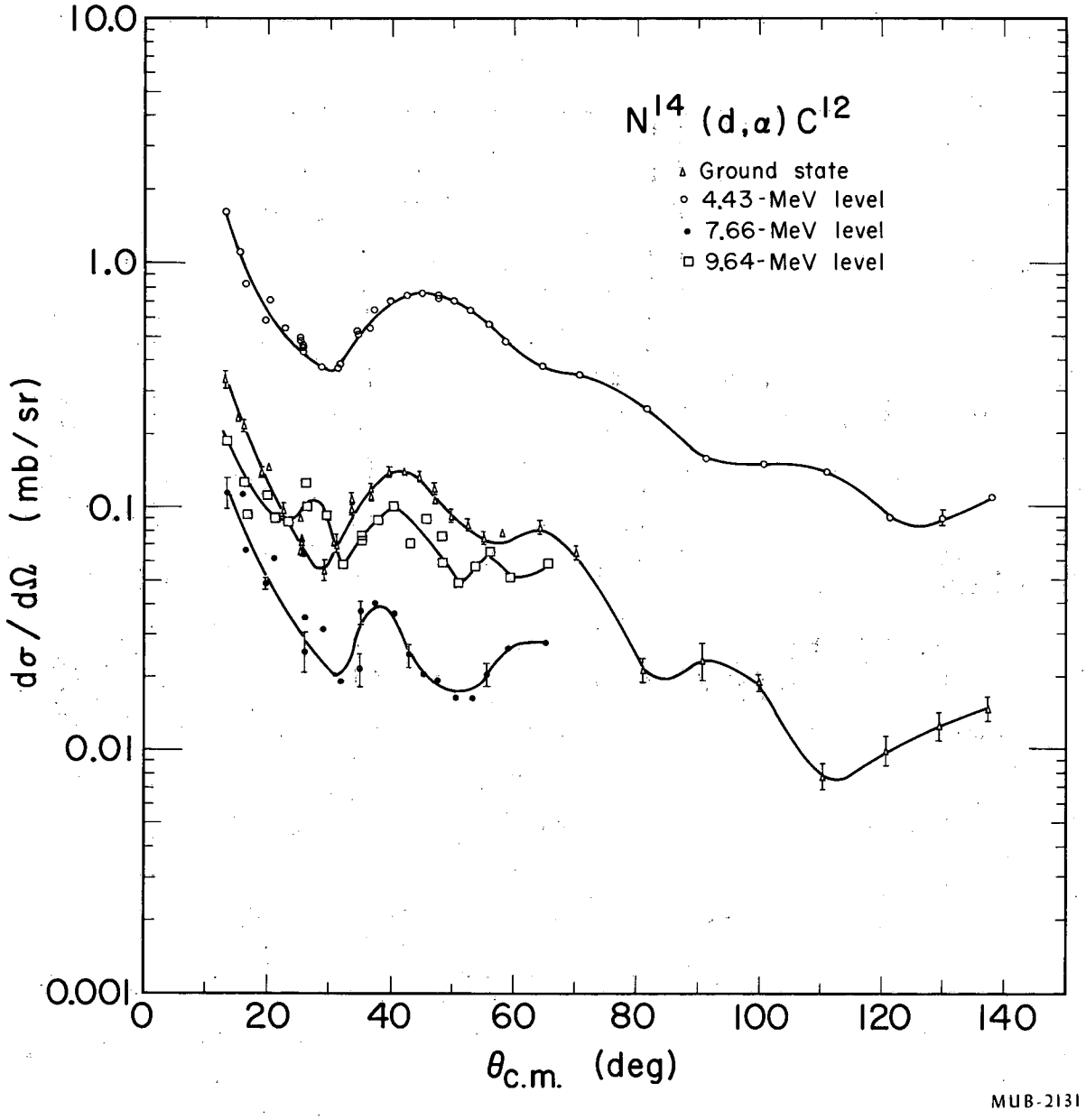
N14 (d,α) C12
Ground state
4.43-MeV level
7.66-MeV level
9.64-MeV level
10.0
1.0
0.1
0.01
0.001
dσ/dΩ (mb/sr)
0
20
40
60
80
100
120
140
θc.m. (deg)
MUB-2131

Fig. 11

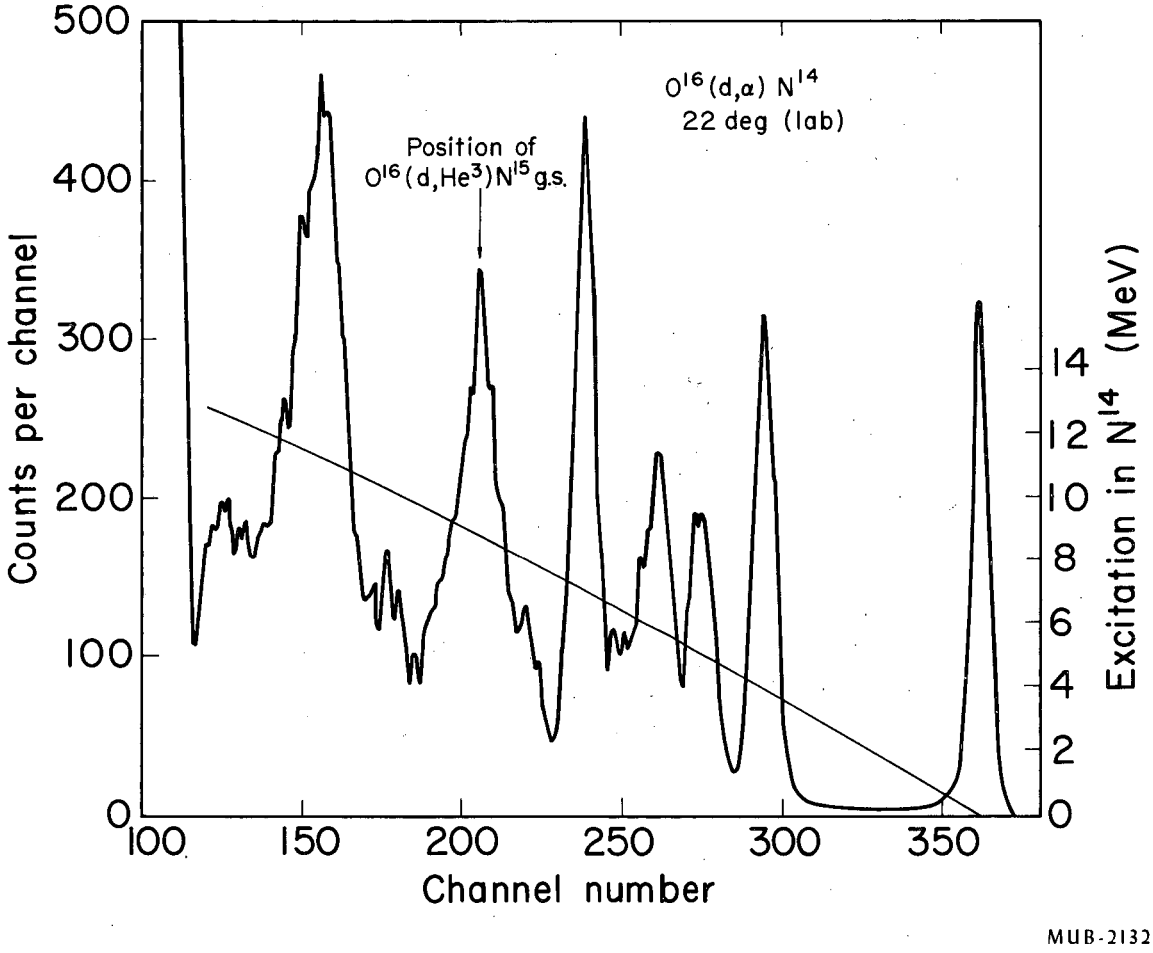
500
400
300
200
100
0
Counts per channel
100
150
200
250
300
350
Channel number
Position of
O16(d,He3)N15 g.s.
O16(d,α) N14
22 deg (lab)
14
12
10
8
6
4
2
0
Excitation in N14 (MeV)
MUB-2132

Fig. 12

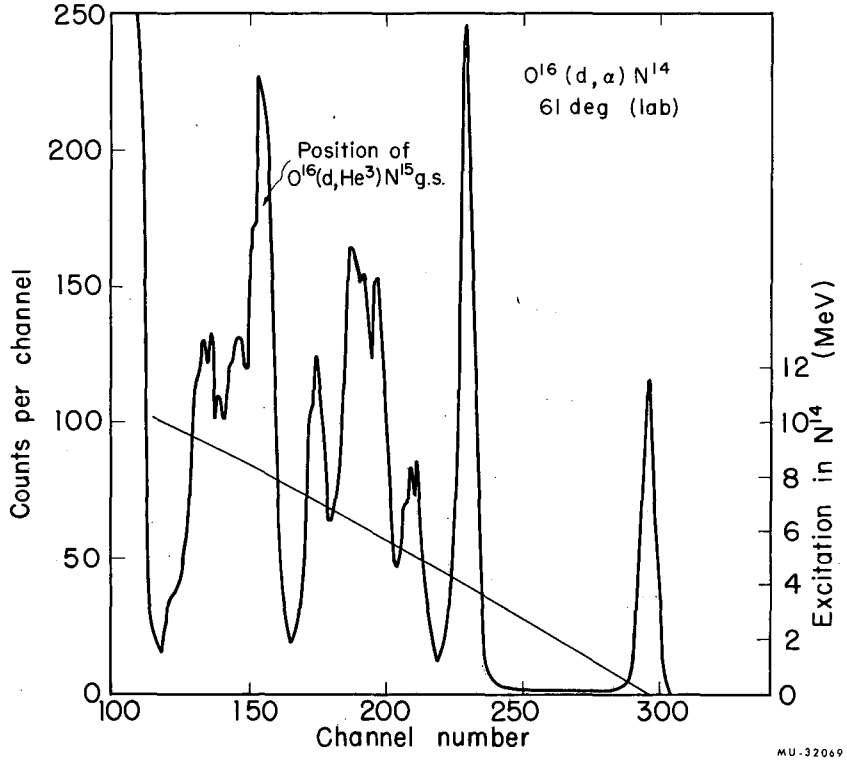
250
200
150
100
50
0
Counts per channel
100
150
200
250
300
Channel number
$O^{16}(d,\alpha)N^{14}$
61 deg (lab)
Position of
$O^{16}(d,He^3)N^{15}$g.s.
12
10
8
6
4
2
0
Excitation in N^{14} (MeV)
MU-32069

Fig. 13

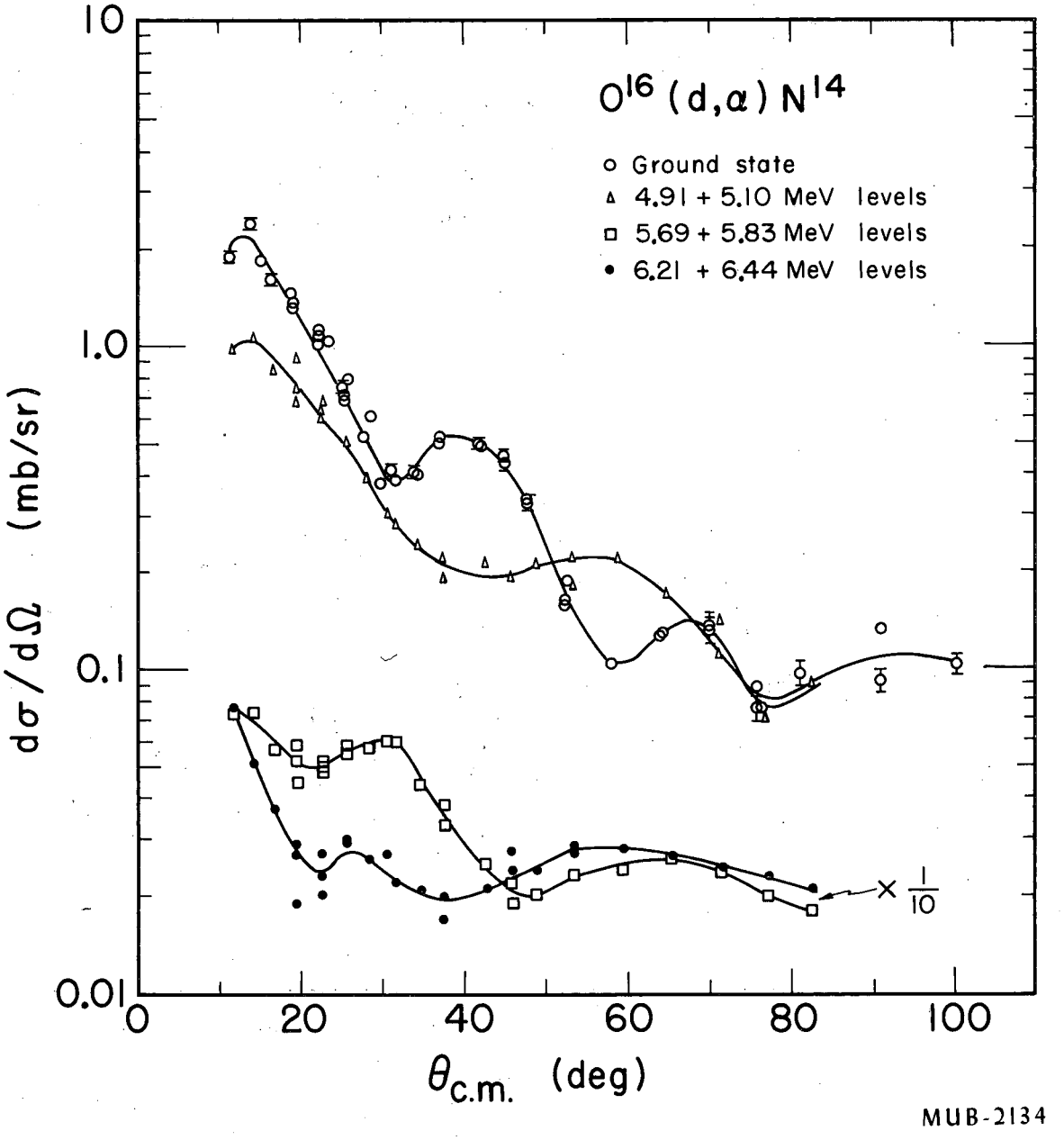
$O^{16}(d,\alpha)N^{14}$
Ground state
4.91 + 5.10 MeV levels
5.69 + 5.83 MeV levels
6.21 + 6.44 MeV levels
10
1.0
0.1
0.01
0
20
40
60
80
100
$d\sigma/d\Omega$ (mb/sr)
$\theta_{c.m.}$ (deg)
× 1/10
MUB-2134

Fig. 14

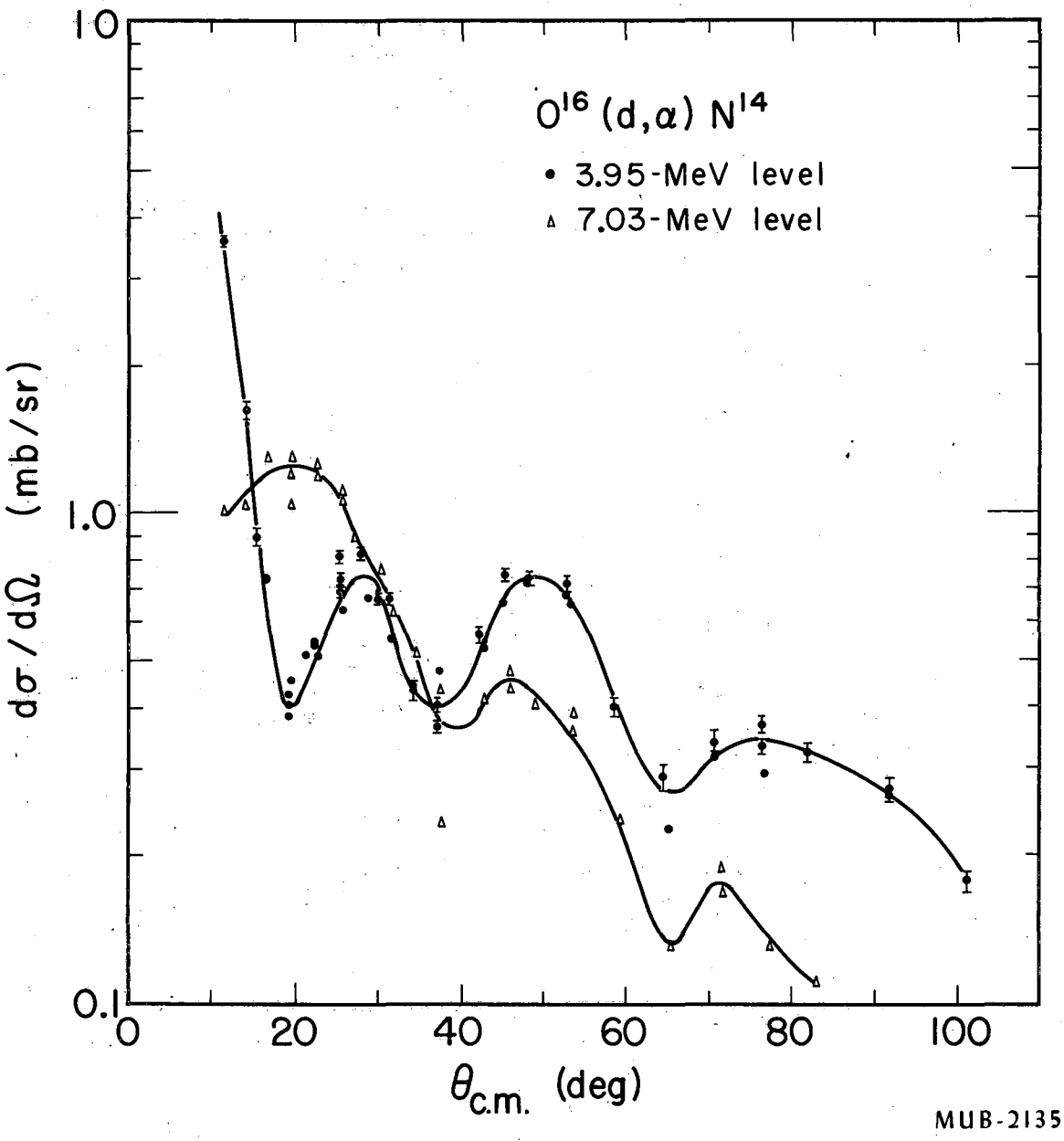
$O^{16}(d,\alpha)N^{14}$
• 3.95-MeV level
▵ 7.03-MeV level
10
1.0
0.1
0
20
40
60
80
100
$d\sigma/d\Omega$ (mb/sr)
$\theta_{c.m.}$ (deg)
MUB-2135

Fig. 15

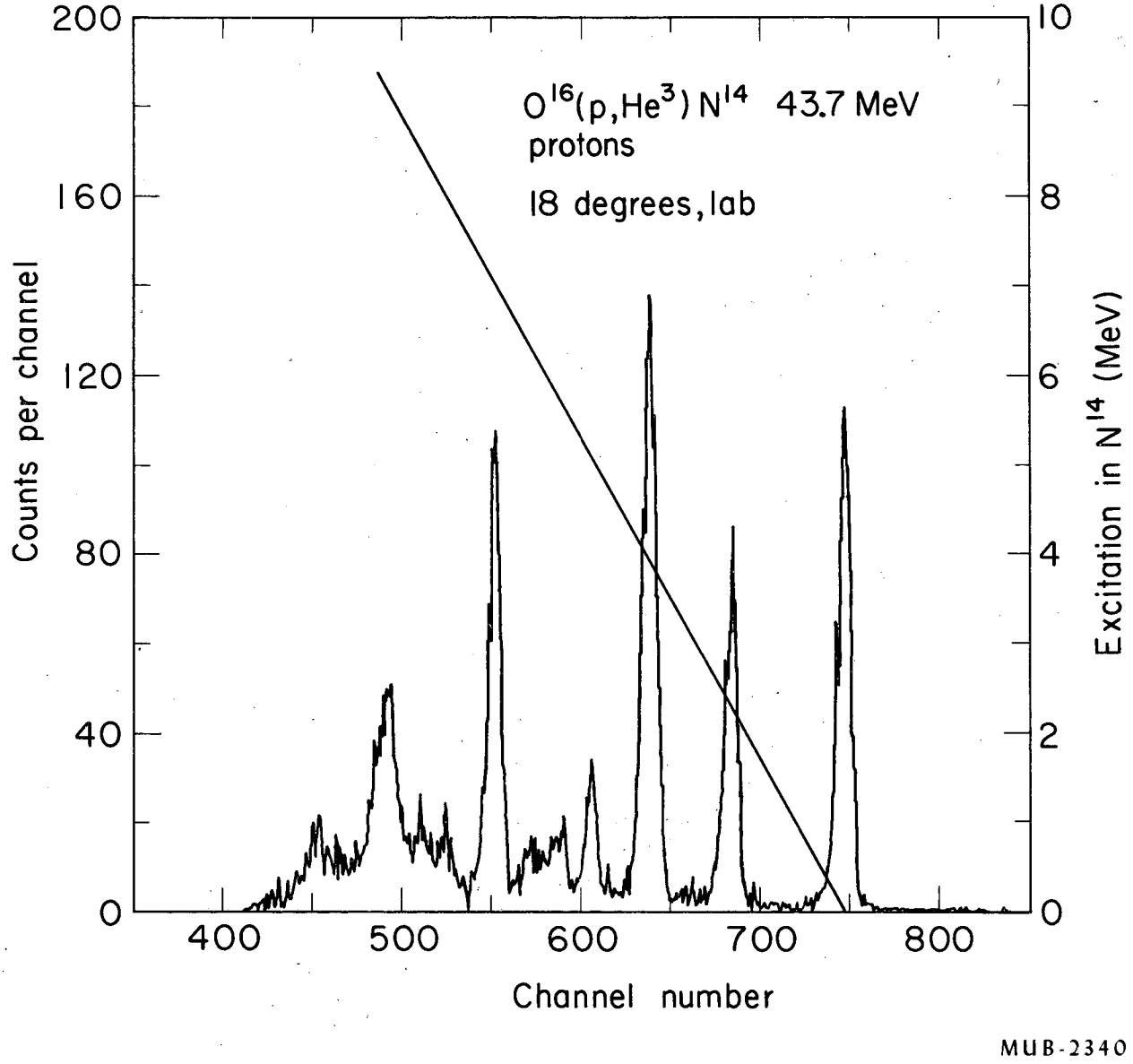

MUB-2340

Fig. 16

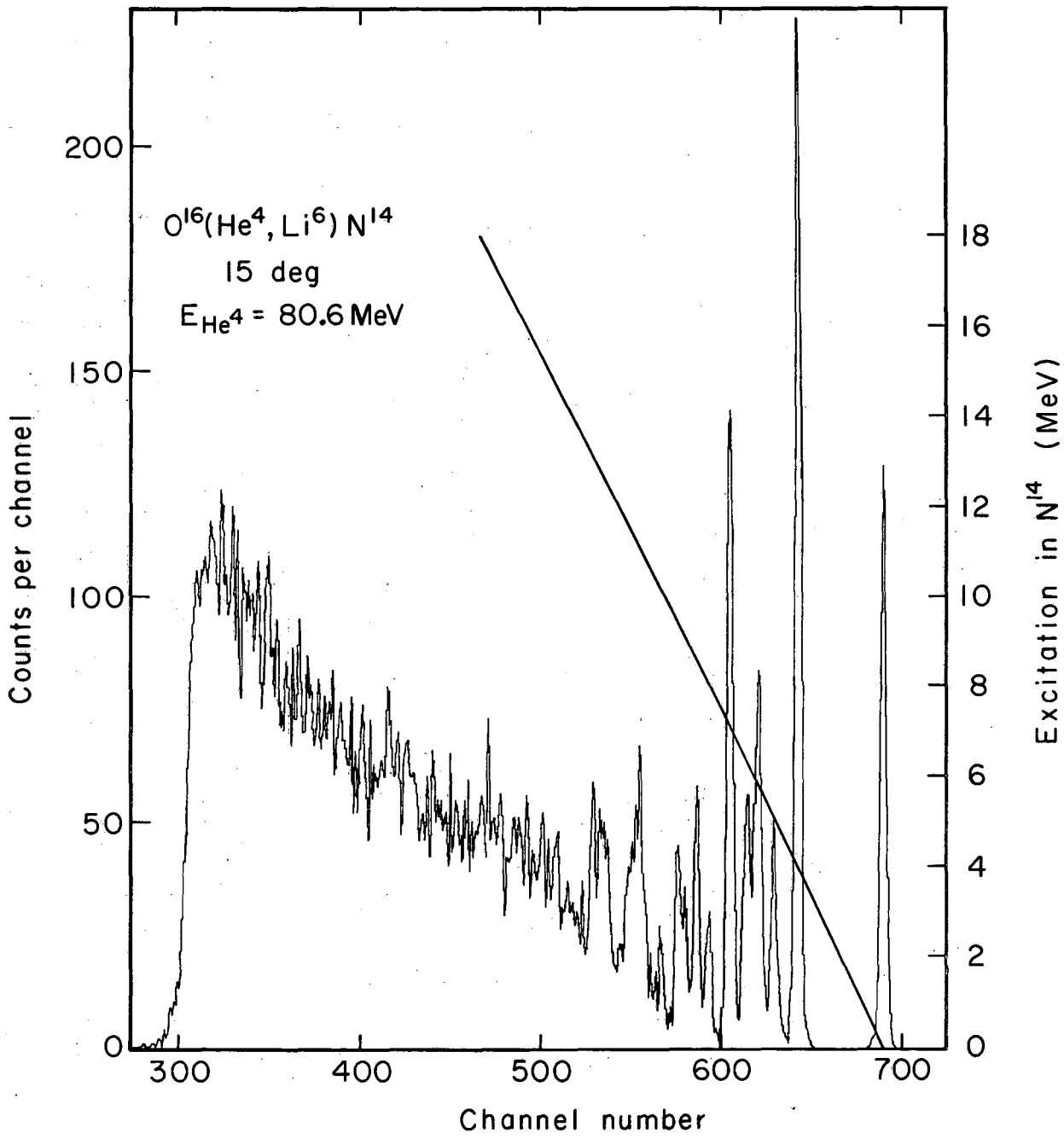

MUB-6134

Fig. 17

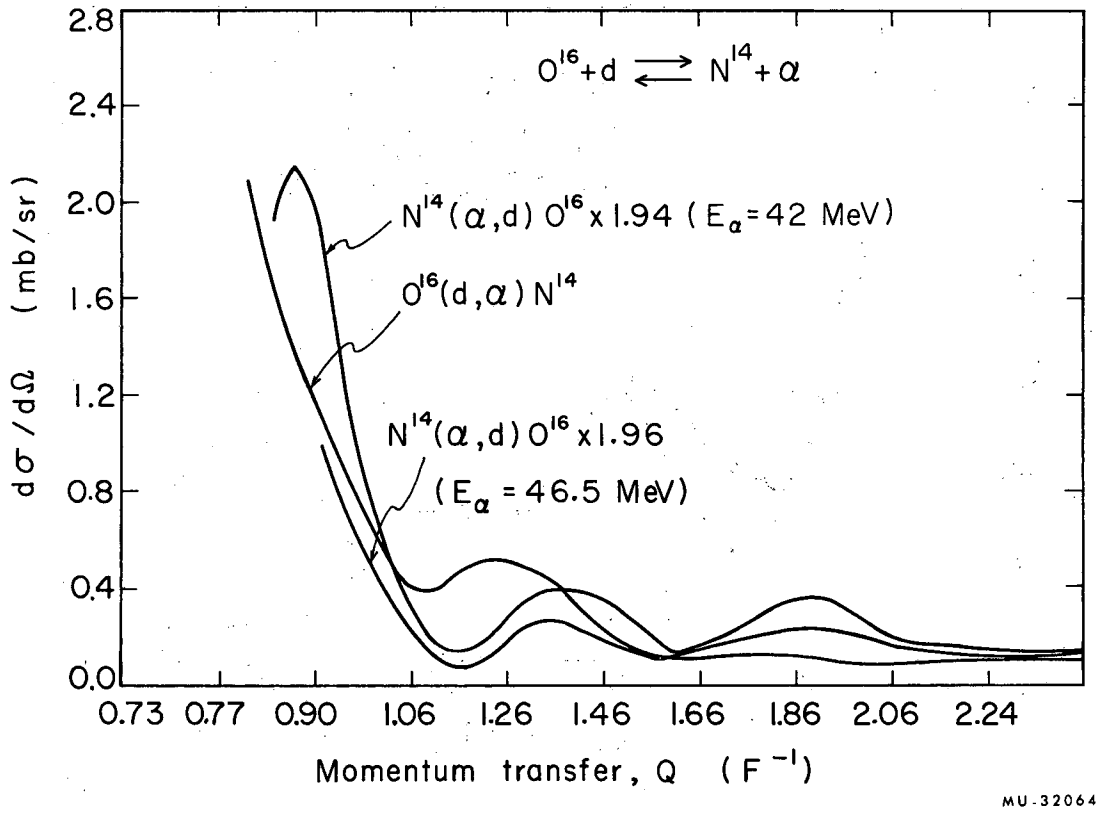
$O^{16}+d \rightleftharpoons N^{14}+\alpha$
$N^{14}(\alpha,d)O^{16} \times 1.94$ (E_α=42 MeV)
$O^{16}(d,\alpha)N^{14}$
$N^{14}(\alpha,d)O^{16} \times 1.96$
(E_α = 46.5 MeV)
$d\sigma/d\Omega$ (mb/sr)
2.8
2.4
2.0
1.6
1.2
0.8
0.4
0.0
0.73 0.77 0.90 1.06 1.26 1.46 1.66 1.86 2.06 2.24
Momentum transfer, Q (F^{-1})
MU-32064

Fig. 18

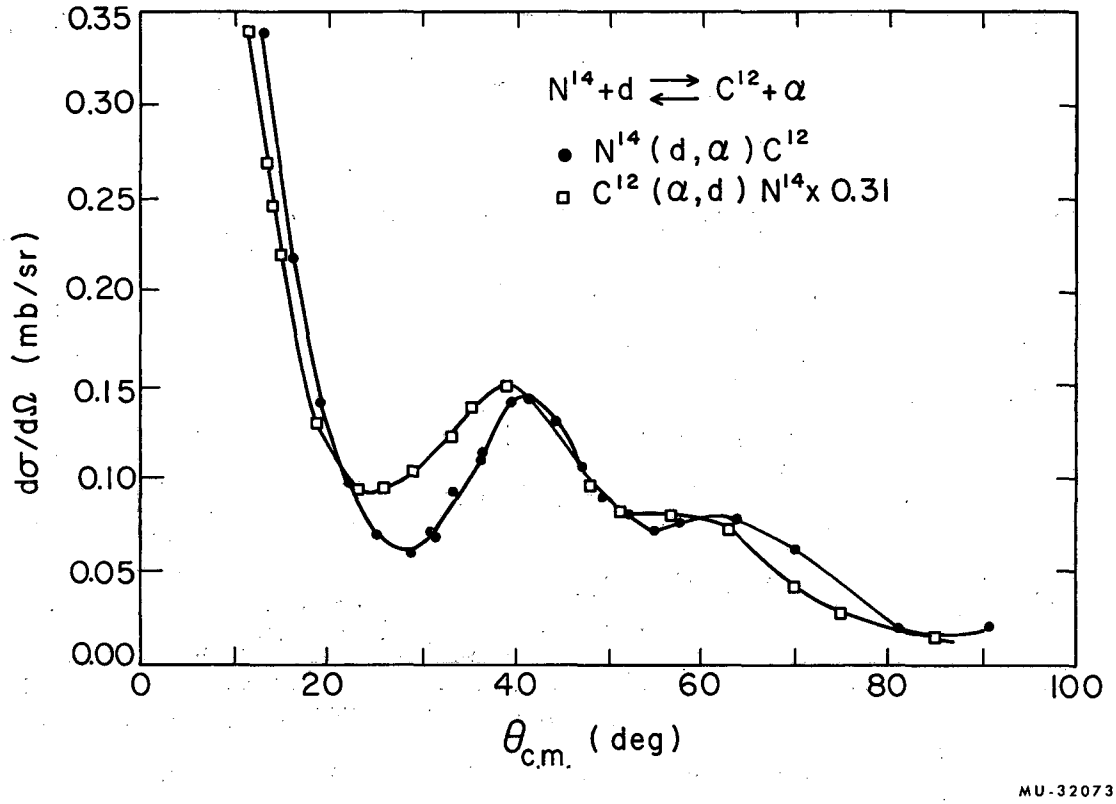
0.35
0.30
0.25
0.20
0.15
0.10
0.05
0.00
dσ/dΩ (mb/sr)
0
20
40
60
80
100
θc.m. (deg)
N14+d ⇌ C12+α
● N14 (d,α) C12
□ C12 (α,d) N14x 0.31
MU-32073

Fig. 19

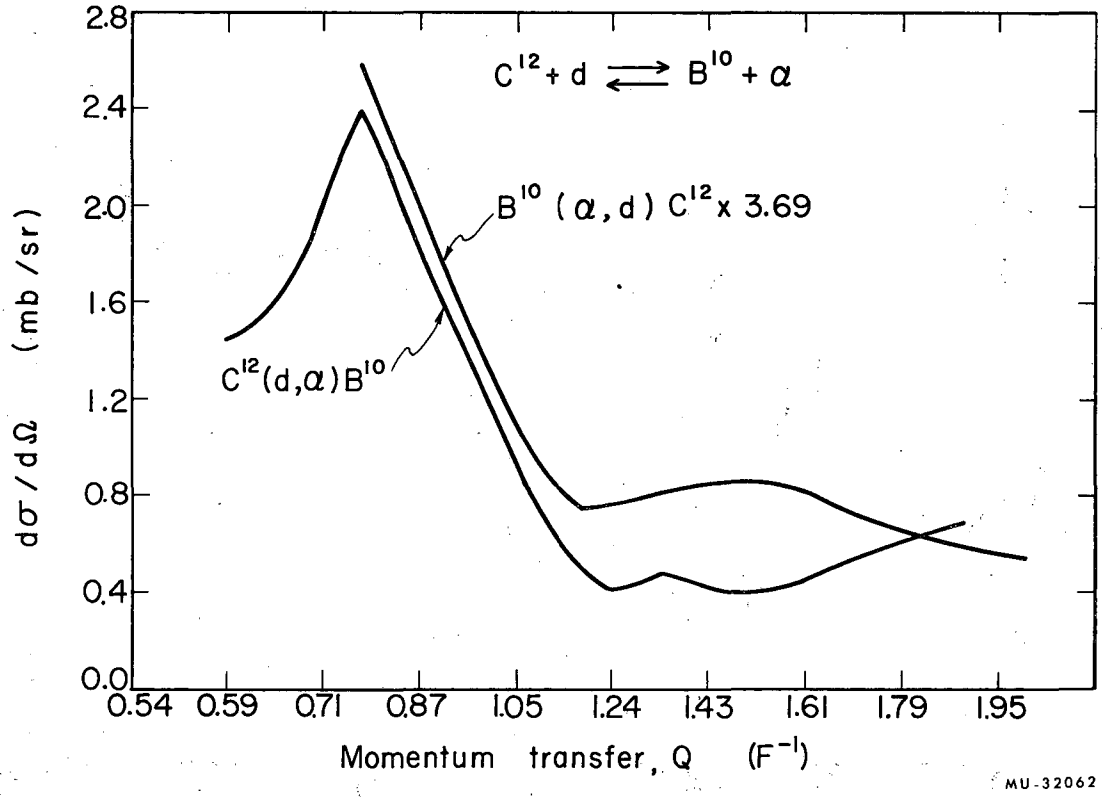
$C^{12} + d \rightleftharpoons B^{10} + \alpha$
$B^{10}(\alpha, d)C^{12} \times 3.69$
$C^{12}(d,\alpha)B^{10}$
$d\sigma/d\Omega$ (mb/sr)
2.8
2.4
2.0
1.6
1.2
0.8
0.4
0.0
0.54 0.59 0.71 0.87 1.05 1.24 1.43 1.61 1.79 1.95
Momentum transfer, Q (F^{-1})
MU-32062

Fig. 20

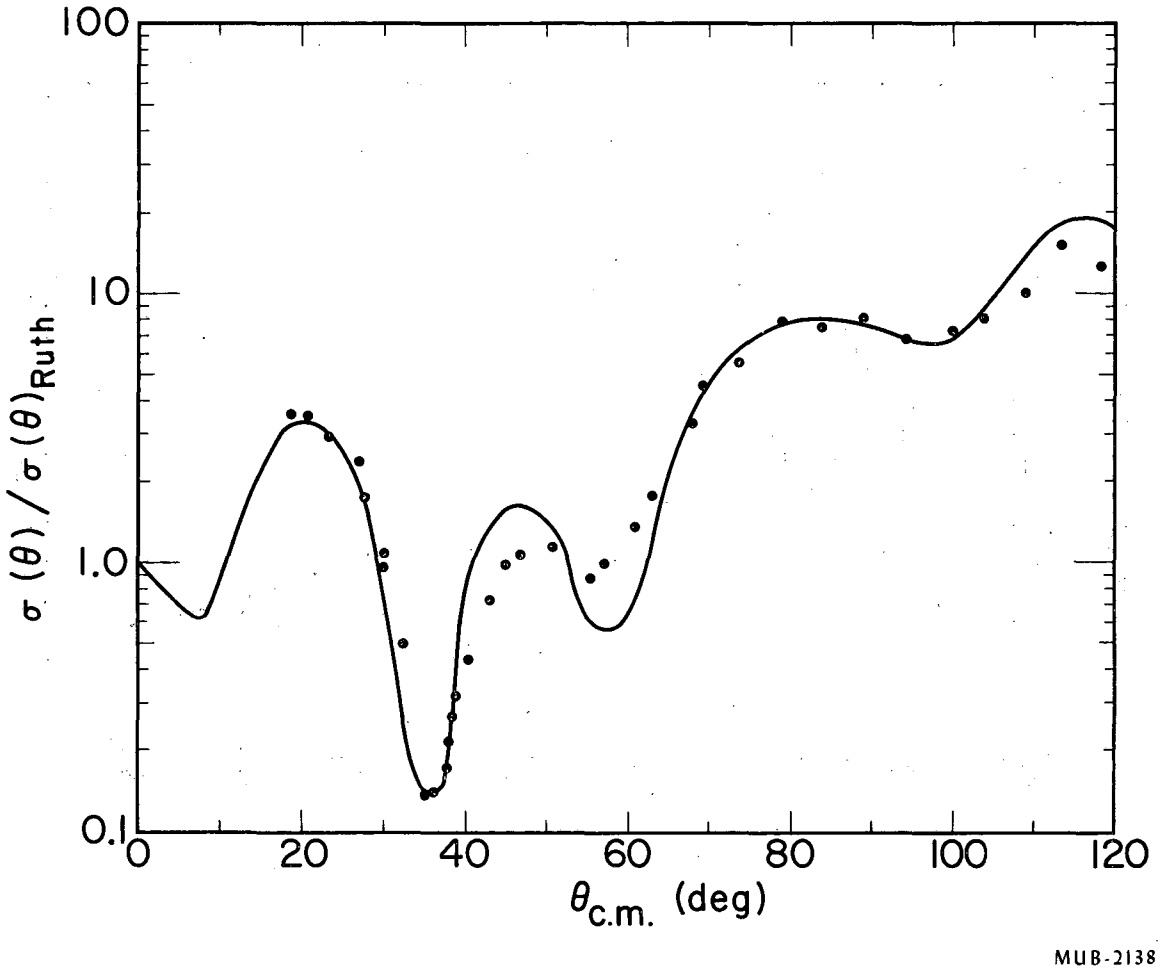
100
10
1.0
0.1
0
20
40
60
80
100
120
$\sigma(\theta)/\sigma(\theta)_{Ruth}$
$\theta_{c.m.}$ (deg)
MUB-2138

Fig. 21

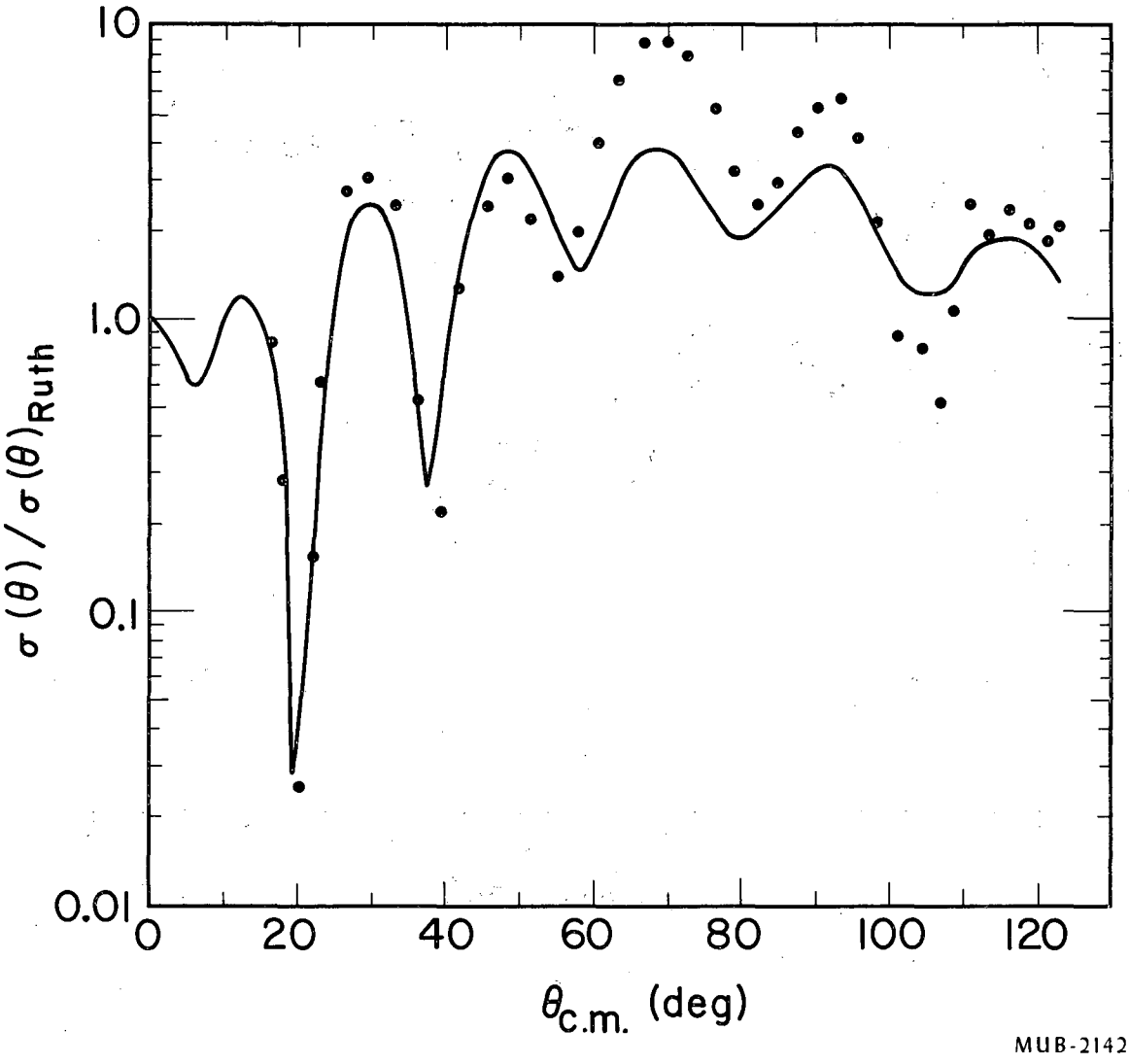

Fig. 22

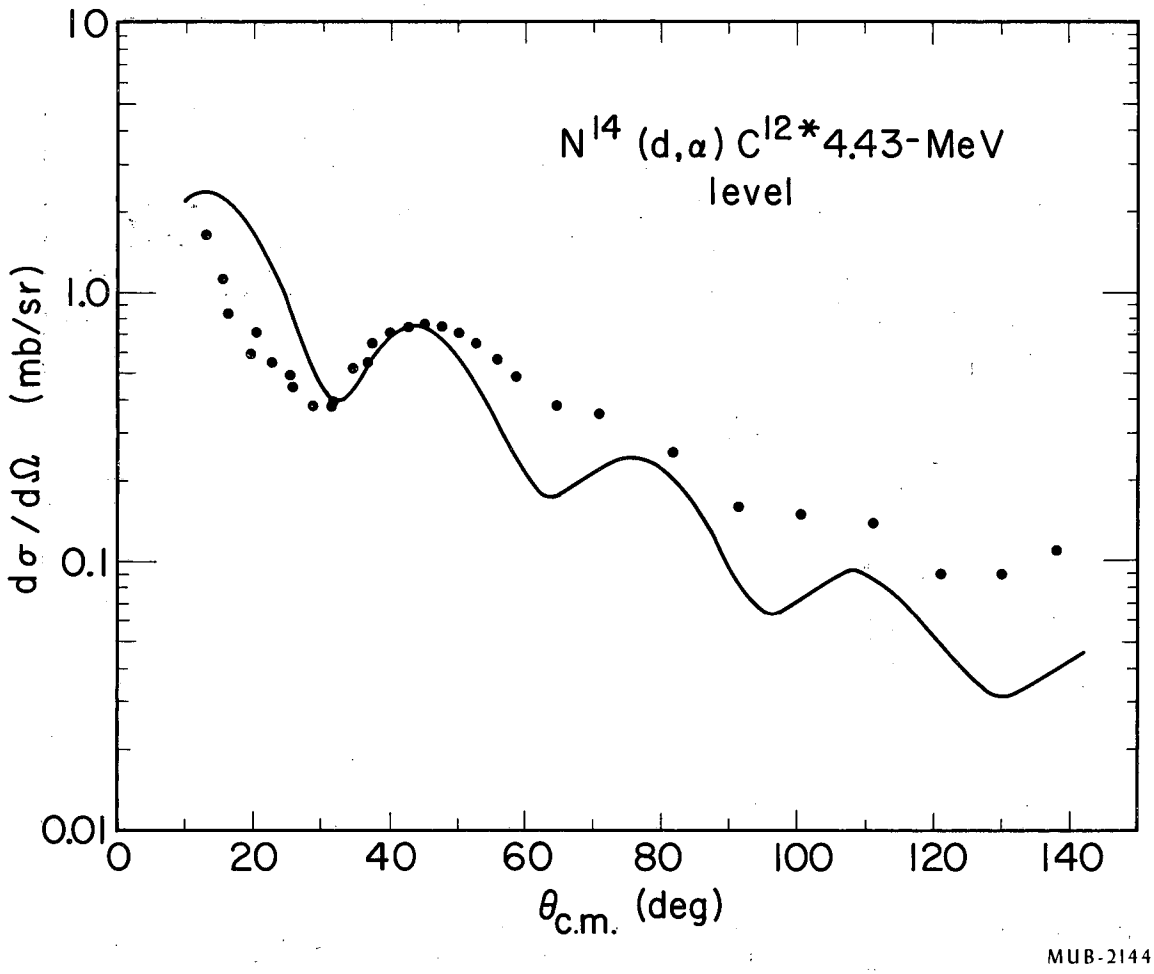
N14 (d,α) C12*4.43-MeV
level
10
1.0
0.1
0.01
dσ/dΩ (mb/sr)
0
20
40
60
80
100
120
140
θc.m. (deg)
MUB-2144

Fig. 23

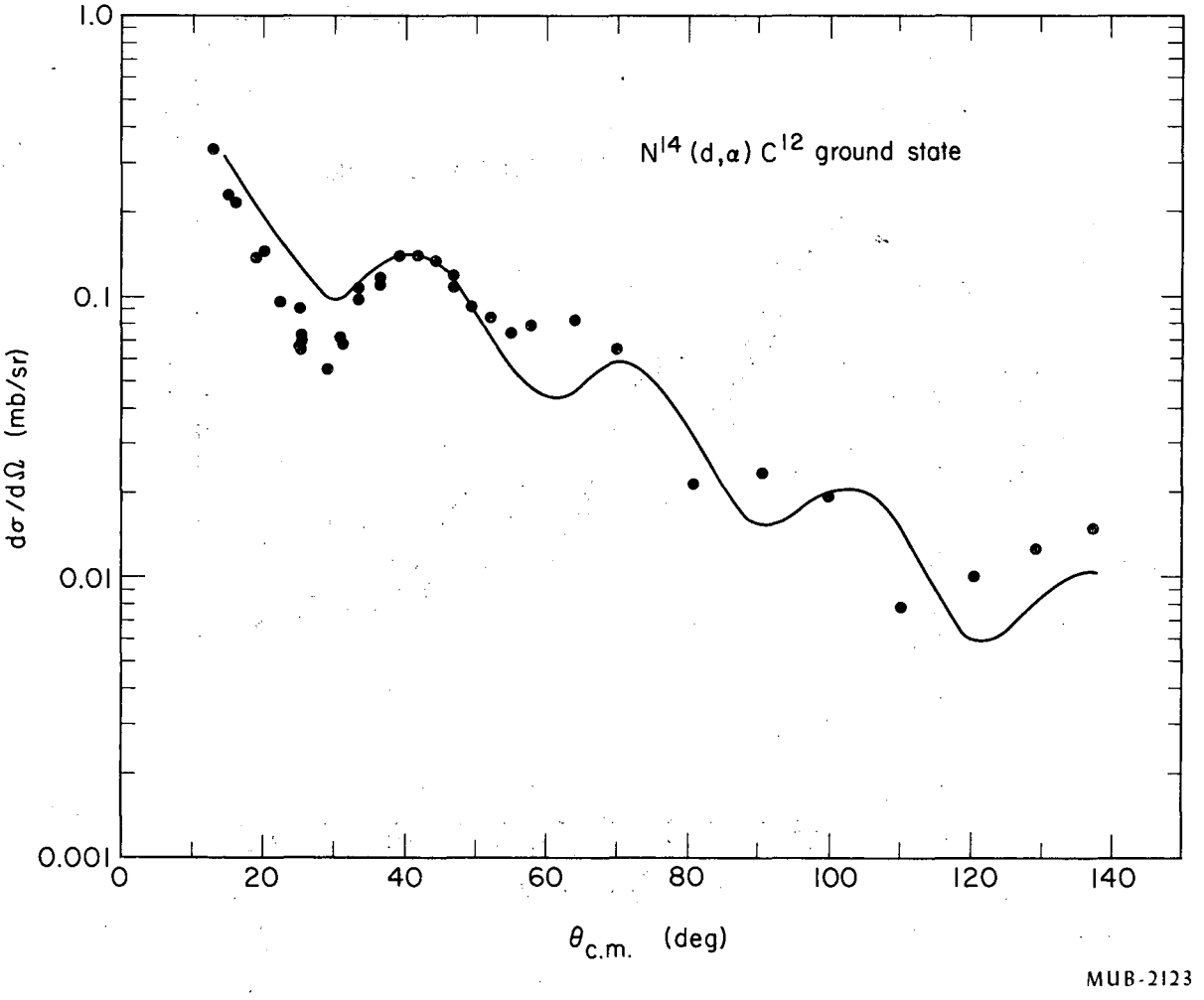
1.0
0.1
0.01
0.001
0
20
40
60
80
100
120
140
$d\sigma/d\Omega$ (mb/sr)
$\theta_{c.m.}$ (deg)
$N^{14}(d,\alpha)C^{12}$ ground state
MUB-2123

Fig. 24

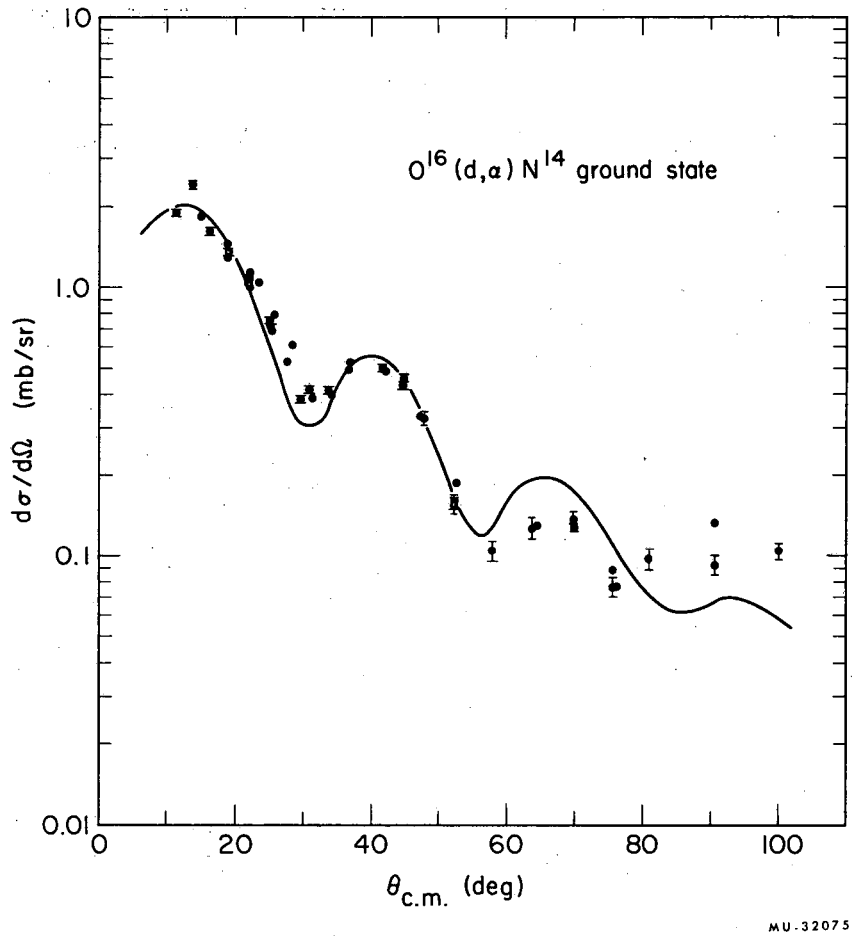
$O^{16}(d,\alpha)N^{14}$ ground state
10
1.0
0.1
0.01
0
20
40
60
80
100
$d\sigma/d\Omega$ (mb/sr)
$\theta_{c.m.}$ (deg)
MU-32075

Fig. 25

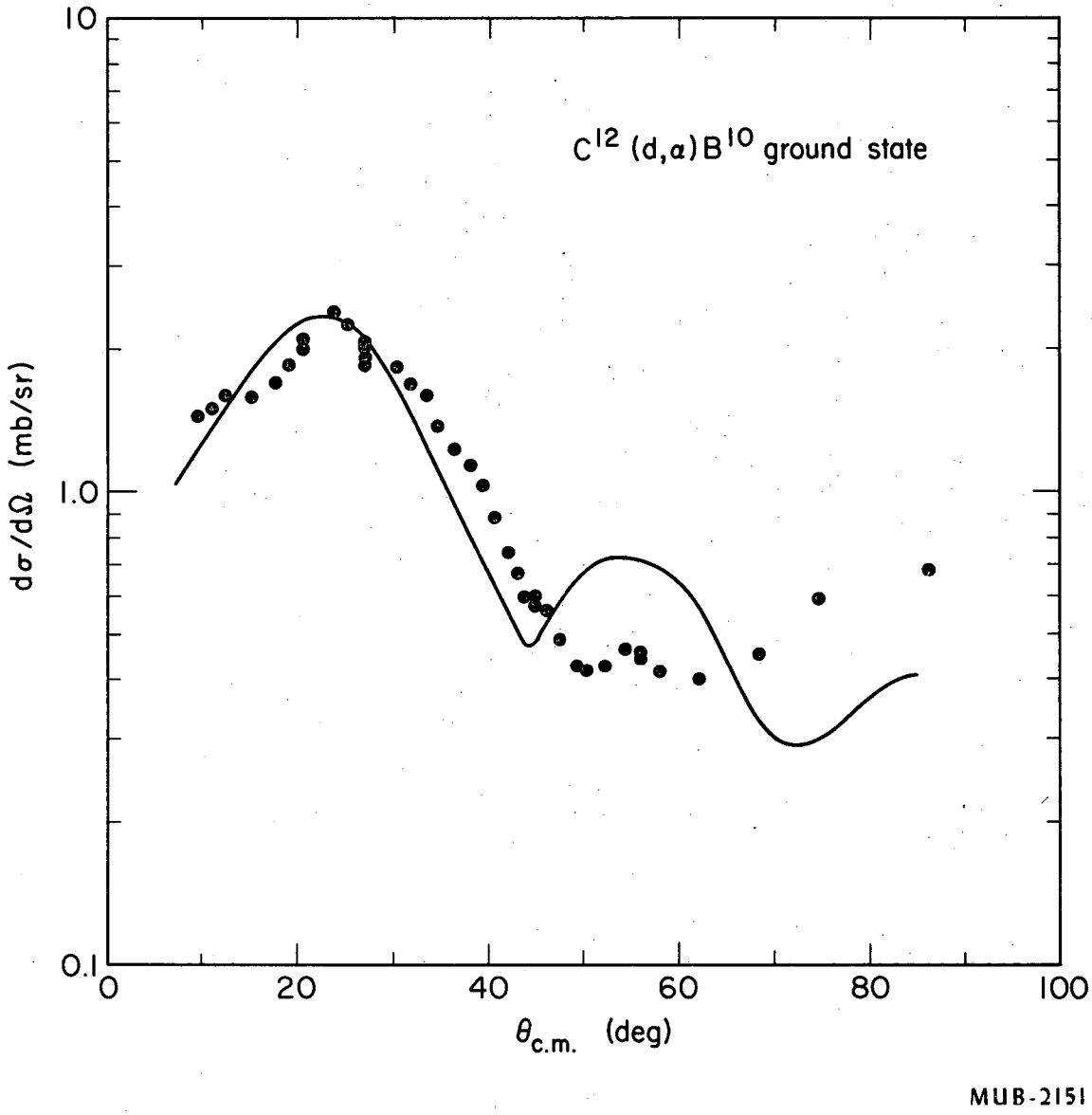
$C^{12}(d,\alpha)B^{10}$ ground state
10
1.0
0.1
0
20
40
60
80
100
$d\sigma/d\Omega$ (mb/sr)
$\theta_{c.m.}$ (deg)
MUB-2151

Fig. 26

This report was prepared as an account of Government sponsored work. Neither the United States, nor the Commission, nor any person acting on behalf of the Commission:

A. Makes any warranty or representation, expressed or implied, with respect to the accuracy, completeness, or usefulness of the information contained in this report, or that the use of any information, apparatus, method, or process disclosed in this report may not infringe privately owned rights; or

B. Assumes any liabilities with respect to the use of, or for damages resulting from the use of any information, apparatus, method, or process disclosed in this report.

As used in the above, "person acting on behalf of the Commission" includes any employee or contractor of the Commission, or employee of such contractor, to the extent that such employee or contractor of the Commission, or employee of such contractor prepares, disseminates, or provides access to, any information pursuant to his employment or contract with the Commission, or his employment with such contractor.